People's Democratic Republic of Algeria

Ministry of Higher Education and Scientific Research

University of Blida-1

Faculty of Technology

Renewable Energies Department

Graduation Dissertation

In view of obtaining the Master's degree in Renewable Energies

OPTION: Photovoltaics Conversion

Theme:

<div style="border:1px solid black; padding:10px;">

Contribution to the Modeling of Photovoltaic Generators

</div>

Presented by: SADAOUI MOHAMMED EL AMIN

Graduated in front of jury composed of:

DOUMAZ Toufik	MAA, Blida 1 University	Chairman
AIT SAHED Oussama	MCB, Blida 1 University	Examiner
BENZETTA Halim	MCB, Ecole Supérieure des Transmissions	Supervisor
BOUKENOUI Rachid	MCB, Blida 1 University	Co-supervisor

Blida, 2023

ملخص :يتم التحقيق في ثلاث تقنيات مختلفة للطاقة الكهروضوئية: (Poly C-Si) Poly-Crystalline Silicon و Copper Indium Gallium Selenide (CIGS) و (CdTe) Cadmium Telluride من حيث عدة جوانب. تم اقتراح نموذج كهروضوئي يعتمد على ورقة البيانات من المصنع. يعتمد هذا النموذج على استخدام إجراء بسيط يأخذ فقط معايير قائمة البيانات في الاعتبار لتحديد مقاومة سلسلة الخلايا الشمسية. علاوة على ذلك، يتم تكييف قيمة عامل المثالية لتناسب تقنية الخلايا الشمسية. تم استخدام كل من مقاومة السلسلة المحددة وقيم عامل المثالية داخل كتلة الخلايا الشمسية التي يوفرها صندوق أدوات Matlab-Simscape بالإضافة إلى برنامج SCAPS 1-D لنمذجة وحدات كهروضوئية مختلفة لها تقنيات مختلفة، بالإضافة إلى التنبؤ بخصائصها التوتر-التيار (I-V) والتوتر- الطاقة ((P-V). يتم استخدام مرفق اختبار لإجراء الاختبارات المطلوبة لتقييم النموذج الكهروضوئي المقترح. تقارن النتائج التجريبية التي تم الحصول عليها في ظل ظروف مناخية مختلفة بنتائج المحاكاة. وتجري المقارنة بتقييم أربعة أخطاء إحصائية بهدف قياس دقة النموذج المقترح في التنبؤ بالخصائص I-V و P-V.

الكلمات المفتاحية : الطاقة الكهروضوئية , Simscape , SCAPS 1-D , الخلايا الشمسية ,النموذج الكهروضوئي.

Abstract: In this dissertation, three different PV technologies: Poly-Crystalline Silicon (Poly C-Si), Copper Indium Gallium Selenide (CIGS) and Cadmium Telluride (CdTe) are investigated in terms of several aspects. A PV model based on Manufacture's Datasheet has been proposed. It is based on the usage of a simple procedure which takes only the datasheet parameters into consideration to identify the series resistance of solar cells. Moreover, the ideality factor value is adapted to fit the solar cell technology. Both the identified series resistance and the ideality factor values have been used within the solar cell block provided by Matlab-Simscape toolbox as well as SCAPS 1-D Software to model different PV modules having different technologies, as well to predict their characteristics (Current–Voltage (I-V) and Power–Voltage (P-V)). A test facility is employed to carry out the required tests for assessing the proposed PV model. Obtained experimental results under different climate conditions are compared with simulated ones. The comparison is carried out by evaluating four statistical errors with a view of measuring the accuracy of the proposed model in predicting the I-V and P-V characteristics.

Keywords: PV technology, SCAPS 1-D, thin film, Simscape, conversion efficiency, PV modeling.

Résumé: Dans cet thèse, trois technologies PV différentes : le Silicium Polycristallin (Poly C-Si), le Séléniure de Gallium (CIGS) et le Tellure de Cadmium (CdTe) sont étudiés sous plusieurs aspects. Un modèle PV basé sur la fiche technique a été proposé. Son originalité réside dans l'utilisation d'une procédure simple qui ne prend en compte que les paramètres de la fiche technique pour identifier la résistance-série des cellules solaires. De plus, la valeur du facteur d'idéalité est adaptée à la technologie des cellules solaires. La résistance-série identifiée et les valeurs du facteur d'idéalité ont été utilisées dans le bloc de cellules solaires fourni par Matlab-Simscape toolbox ainsi que le logiciel SCAPS 1-D pour modéliser différents modules PV ayant différentes technologies, ainsi que pour prédire leurs caractéristiques (Courant–Tension (I-V) et Puissance–Tension (P-V)). Un banc d'essai est utilisée pour effectuer les essais requis pour évaluer le modèle PV proposé. Les résultats expérimentaux obtenus dans différentes conditions climatiques sont comparés à des résultats simulés. La comparaison est effectuée en évaluant quatre erreurs statistiques en vue de mesurer la précision du modèle proposé dans la prévision des caractéristiques I-V et P-V.

Mots-clés : Technologie photovoltaïque, SCAPS 1-D, couche mince, Simscape, efficacité de conversion, modélisation photovoltaïque.

Summary

List of Figures

List of Tables

Abbreviations

Abbreviation	Word	Abbreviation	Word
CdTe	Cadmium Telluride	Mono C-Si	Monocrystalline Silicon
CIGS	Copper Indium Gallium Selenide	MPPT	Maximum Power Point Tracking
FF	Fill Factor	Poly C-Si	Polycrystalline Silicon
GaAs	Gallium Arsenide	PV	Photovoltaic
IBSC	Intermediate Band Solar Cells	PVG	Photovoltaic Generator
IPV	Indoor Photovoltaic Cells	PWM	Pulse Width Modulation
I_{SC}	Short-Circuit Current	V_{CO}	Open Circuit Voltage

General Introduction

In recent years, PVsystems have gained significant traction as a sustainable and renewable energy source. As the demand for efficient and reliable solar energy increases, researchers and engineers strive to develop accurate and comprehensive models to simulate and analyze the performance of PV systems. Two commonly used tools for this purpose are the MATLAB SimScape Toolbox and SCAPS 1-D software.

The MATLAB SimScape Toolbox is a powerful and versatile simulation environment that provides a wide range of modeling and simulation capabilities. It allows engineers and researchers to create dynamic models of complex physical systems, including PV systems, using a block diagram approach. With SimScape, users can easily integrate electrical, mechanical, thermal, and other domains into their models, enabling a holistic analysis of PV system behavior.

On the other hand, SCAPS 1-D software is specifically designed for simulating and analyzing the electrical behavior of PV devices and systems. It is based on the numerical solution of the semiconductor device equations and offers advanced features for modeling the physical and electrical properties of various PV cell technologies. SCAPS 1-D provides a detailed insight into the operation of individual solar cells and can be used to study the impact of different parameters on overall system performance.

Both MATLAB SimScape Toolbox and SCAPS 1-D software have their unique advantages and applications when it comes to modeling PV systems. SimScape, with its multidomain capabilities, allows for a comprehensive system-level analysis, taking into account various factors such as temperature, shading, and dynamic effects. On the other hand, SCAPS 1-D software focuses on the electrical behavior of individual PV cells, enabling a more detailed understanding of device-level phenomena and material properties.

In this study, we aim to compare the modeling capabilities and performance of a PV system using MATLAB SimScape Toolbox and SCAPS 1-D software. By conducting a thorough analysis and evaluation, we intend to highlight the strengths and limitations of each tool and provide insights into their suitability for different aspects of PV system design and optimization. The findings of this study will contribute to the advancement of PV modeling techniques and support the development of more efficient and reliable solar energy systems.

Overall, the comparison between the Simscape model and the Scaps model in the context of PV system modeling promises to offer valuable insights into the design, analysis, and optimization of solar energy systems, paving the way for more sustainable and environmentally friendly energy solutions.

Our submission is composed of four chapters:

The First chapter deals with the general aspects of solar energy, the operating principle, the advantages and disadvantages of PV systems.

In the Second chapter, we present the modeling of three different PV modules (Q.Smart 95Wp, First Solar FS-272, Q.Pro 230Wp) with three different solar cell types (CIGS,CDTE,Multi-Crystallin) using SCAPS 1-D software.

In the Third chapter, we provide the modeling of the last mentioned PV modules using Simscape from MATLAB.

In the Fourth chapter we are going to compare the results provided by the Simscape model to the ones provided by the SCAPS 1-D model to find the model that gives the best performance.

Finally, we conclude this study with a general conclusion that summarizes the results obtained.

Chapter 1 A General Overview about Photovoltaics

1.1 Introduction

PV solar energy is obtained from the direct conversion of solar radiation into electrical energy. This energy is one of the main sources of renewable energy that has aroused great interest in recent years, it is a source of energy accessible to all (industrial, communities and individuals).

1.2 solar energy

Solar energy is an energy source that depends on the sun. It falls into the category of renewable energy since it is considered inexhaustible. It is also said that it is 100% green because its production does not directly emit CO2.

The deserts of our planet receive in six hours more energy from the sun than humanity consumes in a year. Solar energy is produced and used in several ways:

1.2.1 Solar Thermal energy:

This simply generates heat through a dark panel. We can also use the sun's heat to generate steam, which is then converted into electricity. Solar thermal energy is also used to power:

- A solar heating

- A water heater

- A stove

1.2.2   Solar PV energy:

PV solar energy is obtained by the energy of the sun's rays.

This is the reason why the PV panels that will harvest them, are installed on the roofs, Is to collect photons from the sun, and then make electricity.

1.3 Solar radiation

Electromagnetic radiation consists of "grains" of light called photons. The energy of each photon is directly related to the wavelength λ by the following relation **[3].**

$$Ep = \frac{h * c}{\lambda}$$

$$h = 6.62 * 10^{-34} JS^{-1}$$

$$c = 3 * 10^8 \, mS^{-1}$$

λ is a wave-length propagation that varies between 0.2 and 4*10 mm **[3].**

Without needing a physical support to develop, it accesses the ground after the destruction of a very large amount of its energy, through an area of ultraviolet radiation that is absorbed.

The energy associated with this solar radiation breaks down approximately as follows **[4]:**

- 9% in the ultraviolet band (0.8 µm).

- 47% in the visible band (0.4 to 0.8 µm).

- 44% in the infrared band (>0.8 µm).
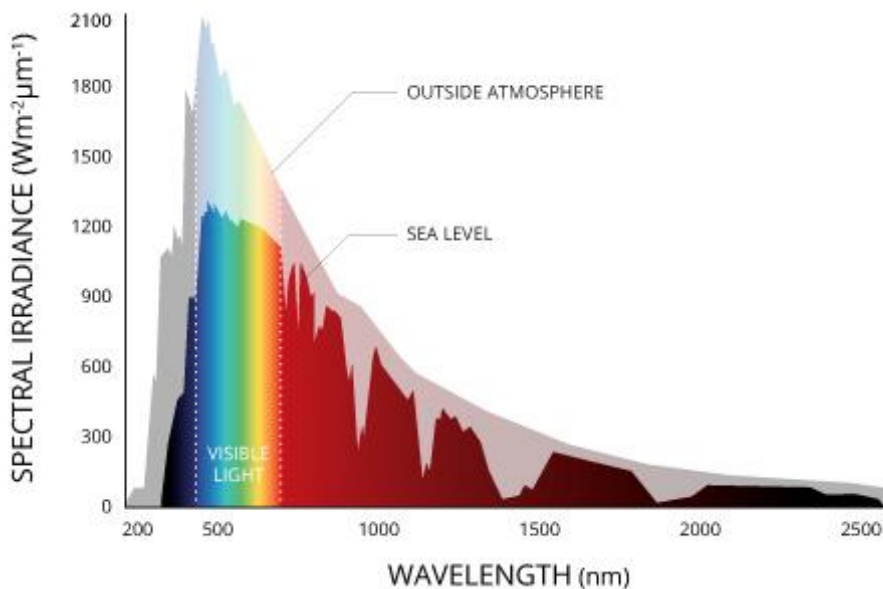
Figure 1.1 : Spectra of the average incoming solar radiation at the top of the atmosphere (red curve) and on the earth's surface (yellow). The fraction of radiation absorbed in The atmosphere is blue, the one that is backscattered in violet **[4]**

1.3.1 Types of Solar radiation
There are four types of radiation:

1.3.1.1 Direct Radiation
Direct radiation is the solar radiation that reaches the earth's surface directly from the sun, without diffusion through the atmosphere. Pyrheliometer is a device that measures the density of direct radiation. The pyrheliometer must be equipped with a device to direct it continuously towards the sun.

1.3.1.2 Diffuse Radiation
It consists of light diffused by the atmosphere (air, cloud cover, aerosols). Dispersion is the phenomenon of division of parallel rays into a number of rays Go in a different direction. It can be measured by a pyranometer with a screen that blocks the sun.

1.3.1.3 Reflected solar radiation

This albedo can be important when the soil is particularly reflective (water, snow). It is characterized by a coefficient proper to the nature of the bond called Albedo 0.

1.3.1.4 Global Reach

Global radiation is the sum of all radiation received, including radiation reflected from the ground and objects on its surface. It is measured by a pyranometer or solarimeter without a screen. Weather stations generally measure horizontal global radiation by a horizontal pyranometer in the required location **[3].**

1.4 PV Energy

1.4.1 History of PV energy

This section presents the history of PVs, its history shows that the use of this energy is very old **[5].**

- **1839 :** French physicist Edmond Becquerel discovers PV effect.
- **1875 :** Werner Von Siemens presents an article on PV effects to the Berlin Academy of Sciences.
- **1954 :** Three American researchers Chapin, Pearson and Prince build a PV cell.
- **1958 :** a solar cell with a performance of 9% developed. The first satellites powered by solar cells were sent to space in the 1960s.
- **1973 :** The first house powered by PV cells was built at the University of Delaware.
- **1983 :** The first PV-powered car travels a distance of 4000 km in Australia in 18 days **.**
- **2013 :** global production of PV modules reached 39.8 Gigawatts.
- **2013 :** The Algerian group Condor Electronics, has launched the production of PV panels whose power varies between 70 W and 285 W.
- **2019 :** PV energy production is available to industry, businesses and individuals, including domestic applications reaching 2.7 % of electricity generated worldwide.

1.4.2 Solar cell

The PV cell or solar cell is an electronic device, which converts solar radiation into electrical energy. The solar cell has major two operations: generation of photogenerated charge carrier (holes and electrons) in absorption layer and separation andcollection of these charge carrier at their respective metal contacts. The working principle is based on the PV effect. Practically for the PV energy conversion of solar radiation, semiconductor materials are used in a form of pn junction. Structure of a solar cell is can be well understood from Figure **1.2** . As discuss in the previous chapter that, the

basic steps in the operation of a solar cell are:

    i.   Generation of photogenerated carriers

    ii.   Generation of current via collection of photogenerated carriers.

    iii.   Generation of a large voltage across the solar cell.

    iv.   Power dissipation at the load.
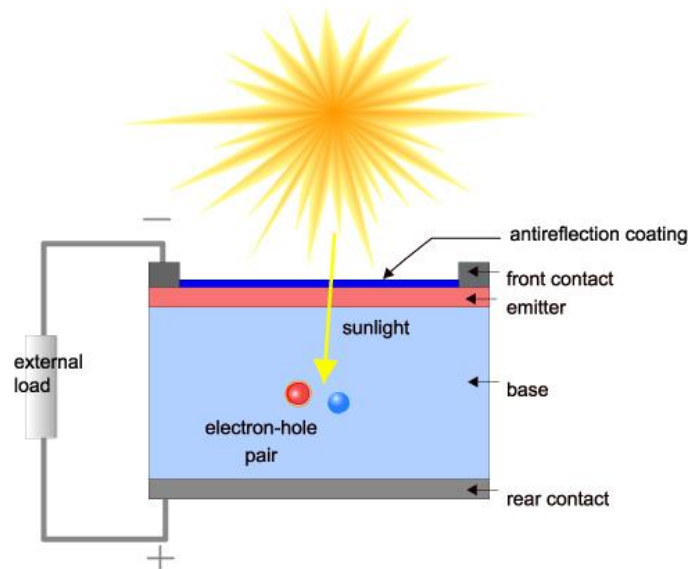
Figure 1.2 : Cross section of solar cell.**[6]**

In Figure I.2 silicon-based solar cell is taken for a better understanding of the construction and working operation of a typical PV cell. p-type silicon works as an absorber layer and n type silicon as a window layer. p-type silicon has the positively charged majority carriers know as holes whereas n-type silicon has the negatively charged majority carriers know as electrons. Both sides of solar cells have conductive surface named as back metal contact and the front metal contact. Photogenerated current flows through the external circuit by using these front and back metal contacts. When solar radiation or photo light falls on the solar cell, carriers (holes and electrons) are generated. These generated carriers are also known as photogenerated carriers and moves towards their respected layers and metal contacts. Due to this, output voltage appears across the solar cell. If we connect the load or any measuring instrument, current flow is started **[6].**

1.4.3   Solar cell historical facts

Energy plays a crucial role in the socio-economic growth of humanity. To fulfill the energy demands,

natural gas, coal, and oil are used. These fossil fuels are too expensive to generate and fulfill the energy demands. Another demerit of using these fossil fuels are the emission of gases or fumes, which disrupts the greenhouse effect and the cause of global warming and also produce soil, air and water pollution. Globally energy demands increase continuously and with the rise in energy production, pollution also increases. The rising energy demands are the main cause of exploring and developing new energy sources. The energy crisis is managed easily by using renewable energy resources. Renewable energy resources are mainly consisting of hydrogen, geothermal, hydropower, solar, wind and biomass sources. These sources are not emitting pollution and help to reduce carbon emission. Solar energy is one of the best renewable energy sources to full fill the energy demands because it's a nature free gift for human mankind. Solar energy provides low- cost, abundant and clean electricity without emitting harmful waste and fumes. PV cells are used for the generation of electricity from solar energy.

American Physical Society explains the history of a solar cell in its publication "APS News" volume 18, issue 4 in April 2009 **[7].** According to APS news antiquity of solar cell is based on French physicist Alexandre-Edmond Becquerel observations of the PV effect in 1839. He was working with metal electrodes in an electrolyte solution. Where he perceived that when the metals were exposed to light then small electric currents were produced but he couldn't explain that effect. In 1873 English engineer named Willoughby Smith testing materials for underwater telegraph cable and discovered the photoconductivity of selenium. Charles Fritts was an American inventor and in 1883 he designed the first selenium based solar cells. He hoped that his solar cells will compete the coal-fired power plant designed by Edison's, but the efficiency of a cell was less than 1% to convert the sunlight energy to electrical energy. So, this design was not very practical.

The next major advancement in solar cell technology was made in 1940 by Russell Shoemaker Ohl, a semiconductor researcher at Bell Laboratories. He was working on silicon samples, one of the samples was crack at the center. He investigated that sample and observed that when light falls on it then current flow started. The cracked was expected to form at the boundaries between the regions containing different levels of impurities, so one side was positively doped and the other one was negatively doped. He made a p-n junction unintentionally, the basics of a solar cell. Ohl patented his solar cell and the conversion efficiency was about 1%. After thirteen years, the first silicon-based practical solar cell was made by scientist's team working at Bell Labs. Engineer Daryl Chapin was working on the telephone power source to use in remote locations in 1953 at Bell Labs. He tried different alternative energy sources and after investigating he got that solar power is one of the most promising power sources for this application.

At the same time, a physicist, Gerald Pearson, and a chemist, Calvin Fuller were working on silicon piece containing impurities of gallium. They dipped silicon piece in lithium, producing a p-n junction.

An ammeter was hooked up to silicon by them and shined the light on it. The ammeter surprised them by jumping significantly. Pearson was already informed of Chapin's work, and he discussed with his friend not to waste time on solar cell of selenium, after that Chapin's, switched to work on silicon. Afterward, they all worked to improve their solar cell properties. They were facing two issues in their work first issue was producing good electrical contacts; the other problem was that over time lithium migrated through the silicon at room temperature and moves away from sunlight. To solve these problems they tried different impurities, finally arsenic and boron were selected these elements created p-n junction stayed close to surface, also they found that with boron-arsenic and silicon cells they can make good electrical contacts. After some other improvements, they linked some solar cells to create a solar battery. On April 25, 1954, Bell Labs announced the invention in Murray Hills, New Jersey. The solar panel was demonstrated by using it to power a solar power radio transmitter and Ferris wheel a small toy. It was a huge improvement of silicon solar cells over earlier solar cells that they were about 6 percent efficient at converting sunlight energy into electricity.

The first silicon solar cell was expensive to produce, and the initial efforts to commercialize were not an enormous success at the beginning. But within a few years, solar cells were used commonly to power satellites and other application. Chapin soon simplified silicon solar cell making process and developed experiment of solar cell science for high school students **[7].**

1.4.4   Generations of solar cells

Traditionally solar cells are separated into three generations.

1.4.4.1 First Generation solar cells

Silicon-based PV cells were the first sector of PVs to enter the market, using processing information and raw materials supplied by the industry of microelectronics. Solar cells based on silicon now comprise more than 80% of the world's installed capacity and have a 90% market share. Due to their relatively high efficiency, they are the most commonly used cells. The first generation of PV cells includes materials based on thick crystalline layers composed of Si silicon. This generation is based on mono-, poly-, and multicrystalline silicon, as well as single III-V junctions (GaAs) **[8,9].**

1.4.4.2 Second Generation solar cells

The thin film PV cells based on CdTe, GaSe, and CIGS or amorphous silicon have been designed to be a lower-cost replacement for crystalline silicon cells. They offer improved mechanical properties that are ideal for flexible applications, but this comes with the risk of reduced efficiency. Whereas the first generation of solar cells was an example of microelectronics, the evolution of thin films required new methods of growing and opened the sector up to other areas, including electrochemistry. **[10].**

1.4.4.3 Third Generation solar cells

The third generation of solar cells (including tandem, perovskite, dye-sensitized, organic, and emerging concepts) represent a wide range of approaches, from inexpensive low-efficiency systems (dye-sensitized, organic solar cells) to expensive high-efficiency systems (III-V multi-junction cells) for applications that range from building integration to space applications. Third-generation PV cells are sometimes referred to as "emerging concepts" because of their poor market penetration, even though some of these have been studied for more than 25 years **[11].**

The latest trends in silicon PV cell development are methods involving the generation of additional levels of energy in the semiconductor's band structure. The most advanced studies of manufacturing technology and efficiency improvements are now concentrated on third-generation solar cells.

One of the current methods to increase the efficiency of PV cells is the introduction of additional energy levels in the semiconductor's band gap (IBSC and IPV cells) and the increasing use of ion implantation in the manufacturing process. Other innovative third-generation cells that are lesser-known commercial "emerging" technologies include **[12]:**

1. Organic materials (OSC) PV cells;
2. Perovskites (PSC) PV cells;
3. Dye-sensitized (DSSC) PV cells;
4. Quantum dots (QD) PV cells ;
5. Multi-junction PV cells ;

1.4.5   Different types of solar cells

Solar cells are divided into two major groups. They are silicon semiconductor type and non-silicon type. The details are as follows.

1.4.5.1 Silicon semiconductor type solar cells

There are three major types of silicon semiconductor PV cells, which are used to create panels.
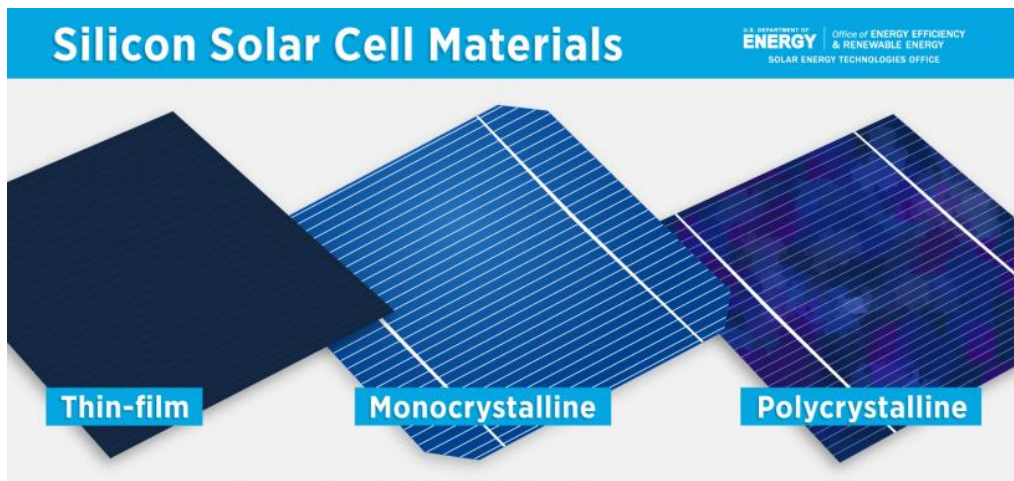
Figure 1.3 : types of silicon semiconductor PV cells **[13]**

1.4.5.1.1   Mono C-Si solar cell

Large (up to 300 mm diameter), cylindrical ingots of extremely pure, single-crystal <u>silicon</u> are grown from molten silicon. The entire ingot is doped, usually p-type with boron, during the melt phase and is sawn into circular wafers less than 0.5 mm thick, from which solar cells are made. According to *Photon International*, such <u>mono C-Si</u> cells supplied 36% of the terrestrial PV market in 2002.

Different manufacturers use variations of the same basic process for making screen-printed cells . Wafer surfaces are etched to form <u>textured surfaces</u> for antireflection and light trapping. Light trapping is implemented to increase the path length within the cell volume for weakly absorbed light at the red end of the spectrum. An n-type <u>dopant</u>, usually phosphorus, is then diffused into the surface to form the p-n junction, producing the in-built electric field to separate the charge carriers. Heavily doped layers are formed at each surface to aid electrical contact and the metal contacts are formed by the screen printing of a metallic paste before firing. <u>Optical coatings</u> may be added to the front surface to further reduce reflection. **[14]**

1.4.5.1.2   Poly C-Si solar cell

Poly C-Si (also called: polysilicon**,** poly crystal, poly-Si or also: multi-Si, mc-Si) are manufactured from cast square ingots, produced by cooling and solidifying molten silicon. The liquid silicon is poured into blocks which are cut into thin plates.The solidification of the material results into cells that contain many crystals, making the surface of the poly-Si/ mc-Si cell less perfect than its mono-Si counterpart. Due to these defects, Poly C-Si cells absorb less solar energy, produce consequently less electricity and are thus less efficient than mono C-Si (mono-Si) cells. Due to their slightly lower efficiency, poly-Si/ mc-Si cells are conventionally a bit larger, resulting in comparably larger PV modules, too. This factor has to be considered if space is limited. Nevertheless, the advantage of poly-Si/ mc-Si cells is that they are easier and thus cheaper to produce**. [15]**

1.4.5.1.3 Amorphous solar cell

Amorphous silicon solar cells are normally prepared by glow discharge, sputtering or by evaporation, and because of the methods of preparation, this is a particularly promising solar cell for large scale fabrication. Because only very thin layers are required, deposited by glow discharge on substrates of glass or stainless steel, only small amounts of material will be required to make these cells. The efficiency of amorphous silicon solar cells has a theoretical limit of about 15% and realized efficiencies are now up around 6 or 7%. If efficiencies of 10% can be reached on large area thin film amorphous silicon cells on inexpensive substrates, then this would be the best approach to produce low cost electricity. **[16]**

1.4.5.1.4 Thin film solar cells

A thin film solar cell is a lightweight and flexible PV device that converts sunlight into electricity. It utilizes thin semiconductor layers deposited on different substrates. Compared to traditional solar cells, thin film solar cells offer cost-effectiveness, versatility, and better performance in low-light conditions. They can be integrated into various surfaces, including curved structures and building facades. However, thin film solar cells generally have lower conversion efficiency compared to their silicon-based counterparts. Additionally, long-term stability and durability can be a concern. The materials commonly used in thin film solar cells include amorphous silicon, cadmium telluride, copper indium gallium selenide, and organic compounds. Ongoing research and development aim to improve the efficiency and stability of thin film solar cell technologies.**[17]**

1.4.6 Current research trends

The power conversion efficiency of different types of solar cells is improved with the passage of time. Primarily semiconductor-based PV devices are of four types such as crystalline silicon ($C - Si$) cells, multijunction cells, thin film technologies-basedcells, and new emerging technologies-based cell. The worldwide research-based different types of PV technologies having the best power conversion efficiencies from 1976 to 2023 are shown in Figure **1.4**. This information chart was published by **NREL** of the United State Department of energy. In a given chart different color schemes shows different technologies, which are given in Table **1.1**. Current trends in the research on thin film technology based PV devices are:

      i. $CIGS$ solar cells

     ii. $CdTe$ solar cells

   iii. $CFTS$ solar cells

   iv.   Kesterite solar cells

v.   Perovskite solar cells

Table 1.1: Device technologies.

No.	Color	Device Type	Description
1		Multi-junction cells	Gallium Arsenide ($GaAs$) Solar panels on spacecraft Concentrator PV
2		Crystalline Si Cells	Single crystal Multi crystalline
3		Thin-Film Technologies	i. Amorphous Si ii. $CIGS$ iii. $CdTe$
4		Emerging PV	$CZT(S, Se)$ based solar cells Dye-sensitized solar cells Quantum dot solar cells Organic solar cells Perovskite solar cells
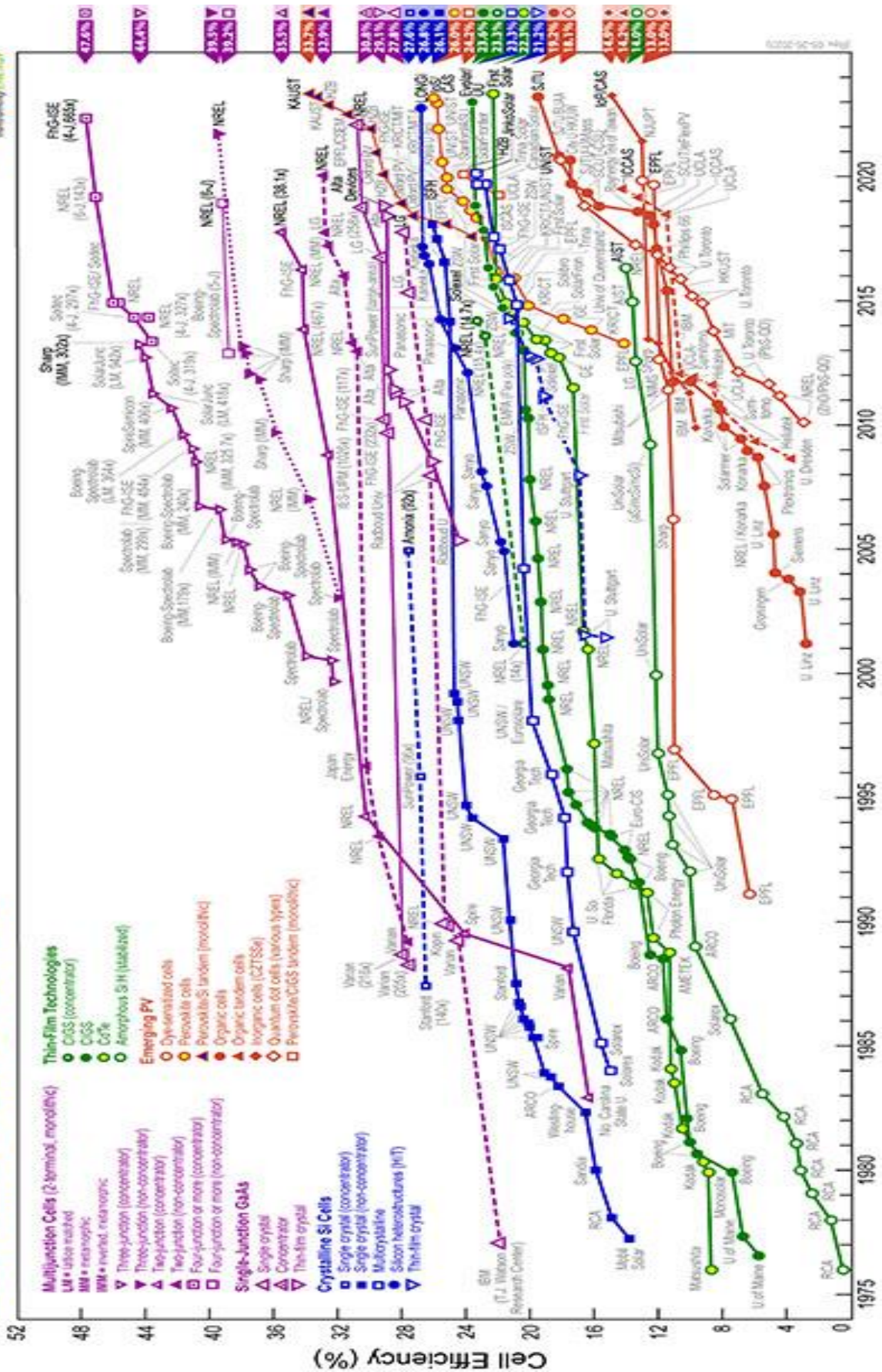
Figure 1.4 : Conversion efficiencies of best research solar cells (*NREL*).[**18**]

1.5 The PV Module

A PV cell is a very low-power generator in comparison with the requirements of the majority of domestic or industrial uses, therefore, PV cells are connected to form a module, and the connection is either in

series to obtain a voltage increase for the same current, either in parallel to increase the current for the same voltage.

The nominal voltage of the module is usually adapted to the 12 volt load and the modules will generally have 36 cells. In addition, the fragility of cells to breakage and corrosion requires protection from their environment and they are generally encapsulated in glass or plastic **[4].**

1.5.1   Characteristic of a Module

There are many parameters to characterize a solar cell.

♣ Peak power, Pc:

The goal sought by the user of a PVG is that the energy produced is as optimal as possible. The electrical power produced by a module varies with the amount of sunlight it can provide, under the following standard measurement conditions:

- Temperature at cell junction is 25°C
- An illumination of 1000 W/m2

♣ Open-circuit voltage, VCO:

The Vco is a voltage at the terminals of the cell when it is not connected to a charge and the absence of any current (I = 0), called open circuit voltage, for "full sun" illumination.

♣ Short-circuit Current, I_{SC} :

Current supplied by a short circuit module (V =0), for "full sun" illumination

♣ Optimum Operating Point, Pm (V_m, I_m):

This is the maximum electrical power that the unit can provide, which is associated with the maximum voltage Vm and the maximum current Im:

Pm = Vm*Im   (I.2)

➕ Efficiency:

The efficiency of a PV cell is the ratio between the amount of light energy converted into electricity and the amount of energy captured by the system. So it is a percentage that allows us to evaluate the efficiency of PV cells.

The higher the percentage, the more electricity the cell produces. This yield has the formula **[3]:**

$$\eta = \frac{Pm}{S*E} \qquad \textbf{(I.3)}$$

➕ Fill Factor:

Used to qualify the quality of the cell and the fill factor is calculated by the ratio between the maximum power and the product of the short circuit current and the open circuit voltage. It is defined by the following relationship:

$$FF = \frac{Pmax}{Isc*Vco} \qquad \textbf{(I.4)}$$

1.5.2 Criteria Affecting PV Module Performance

In order to maintain high-efficiency PV modules, several parameters come into play and affect its reliability, and conversely, can be classified These standards are divided into two:

1.5.2.1 Atmospheric Criteria

These criteria are generally imposed by climatic conditions and depend mainly on the atmosphere and the places of the installations, we can mention several parameters such as lighting, temperature, wind speed, the presence of dust… etc.

➕ The lighting

According to the **formula (I.3)**, we see that the efficiency depends on the illumination, which is variable throughout the day, no action can be taken to increase it, The best solution is to choose a location with strong sunlight to expose the components.

➕ The operating temperature

The increase in temperature directly affects the behavior of solar cells, which produce a voltage drop of about 2 mV per degree, which An increase also leads to a decrease in the maximum available power, So on battery performance.

16

🔸 Non-air criteria

These are independent atmospheric standards, and according to which the efficiency of the module can be improved, including:

🔸 The material of manufacture:

This factor is very important and directly affects conversion PVs, in general, silicon remains the most reliable material The manufacture of this module and its efficiency is the highest.

🔸 The inclination and orientation of the module:

Usually the modules are static. Since the sun is in constant motion, we must give them a direction and a tilt to optimize the annual energy supply. The south orientation of the modules allows maximum light capture during the day and results in production peaks around noon

The tilt angle plays a very important role in attracting the maximum solar flux, and experiments have shown that a module tilt at an angle of 30 degrees is sufficient for better performance.

🔸 Use of load regulators

In order to improve the performance of PV modules and ensure a longer service life, it is necessary to install load regulators, such as serial, parallel, PWM, MPPT.

🔸 Areas of operation of a module

The electrical characteristics of a PV module vary according to temperature, illumination and, in general, operating conditions when connected to a given load. We can break down the characteristic I(v) of a PVG into 3 zones, **Figure 1.5** represents the three essential zones:

The low voltage zone: the current being constant whatever the voltage, for this zone the PVG acts as a current generator and proportional to the irradiation, presenting an internal admittance which can be modeled by 1/ Rsh.

The high voltage zone: which is characterized by a change in the current corresponding to an approximately constant voltage, in this case the generator can be assimilated to a generator of voltage, internal impedance equivalent to the serial resistance RS.

The mid voltage zone: which corresponds to the bend of the characteristic curve, the intermediate zone between the two previous zones, it represents the preferred zone for the generator operation, or the optimal point can be determined, characterized by the torque (Imax/ Vmax).
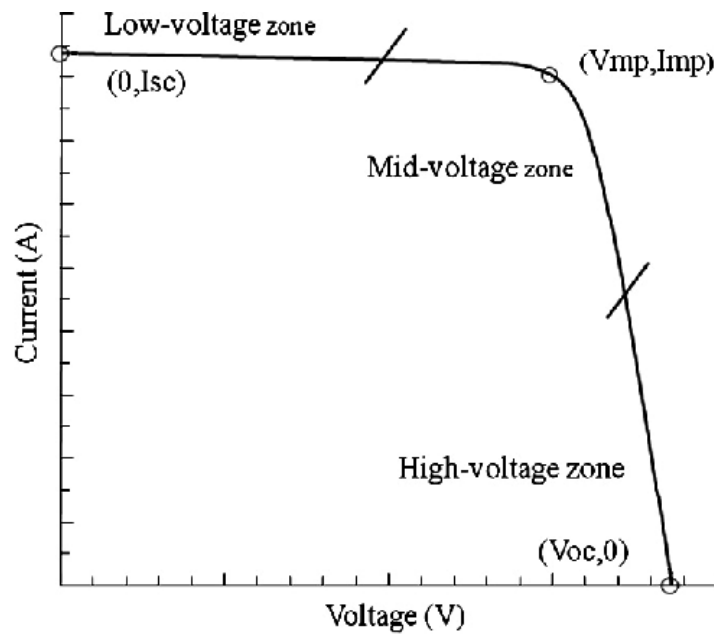
Figure 1.5 : The different zones of I-V characteristic **[20].**

1.6 Photovoltaic Generator

Depending on the application chosen, the term PVG (PVG) is used to designate either one or more PV modules; connected either in series or in parallel.
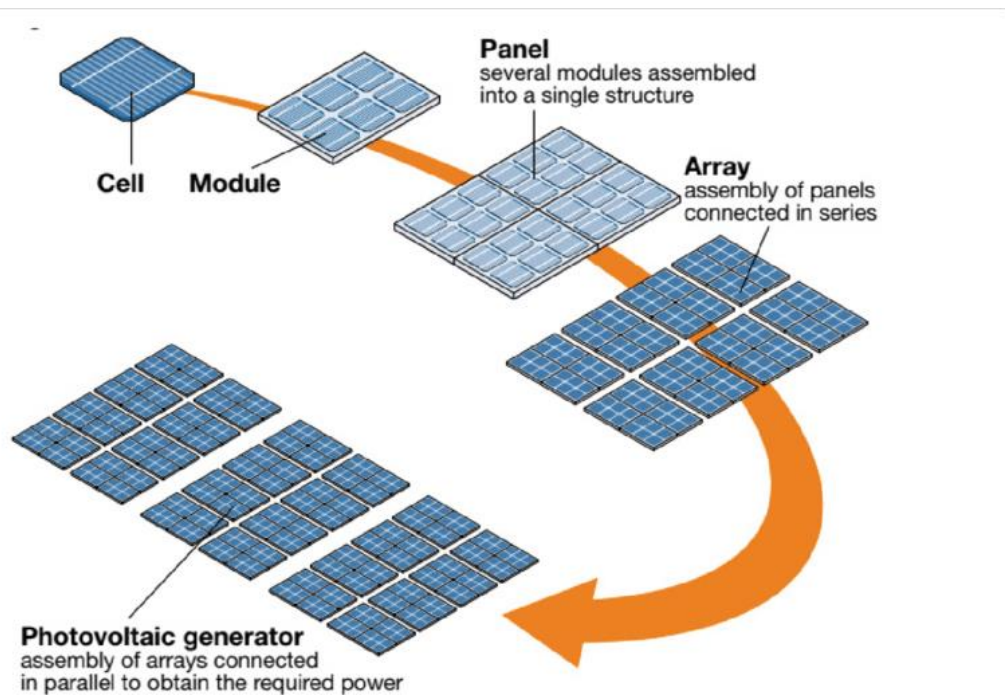
Figure 1.6 : Basic Components of a PVG.**[21].**

If the modules are connected in series, the voltages of each module add up, increasing the overall voltage of the PVG. However, if the modules are connected in parallel, the current increases.

1.6.1   Serialization

A combination of (Ns) modules in series **figure 1.7** increases the voltage of the PVG. The cells are then crossed by the same current and the resulting feature of the series is given by the addition of the elementary voltages of each module. The following equation summarizes the electrical characteristics of a series combination of (Ns) modules.

$$V_{coN_s} = N_s \times V_{co} \tag{I.5}$$

$$I_{ccN_s} = I_{cc} \tag{I.6}$$
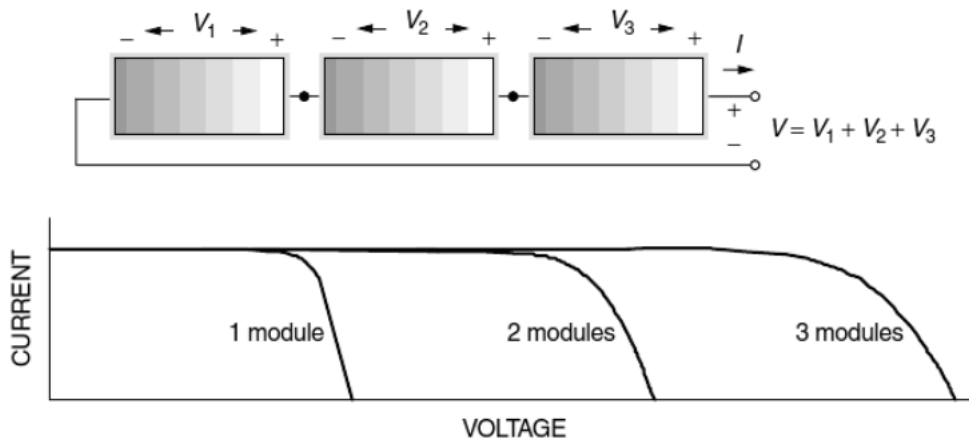
Figure 1.7 : Characteristic current-voltage of Np module in series. **[22].**

1.6.2.   Paralleling:

A parallel combination of (NP) module **figure (1.8)** is possible and increases the generator output current. In a group of identical modules connected in parallel, the modules are subjected to the same voltage and the characteristic resulting from the group is obtained by the addition of currents **.**

$$I_{ccNp} = N_p \times I_{cc} \tag{I.7}$$

$$V_{coNp} = V_{co} \tag{I.8}$$
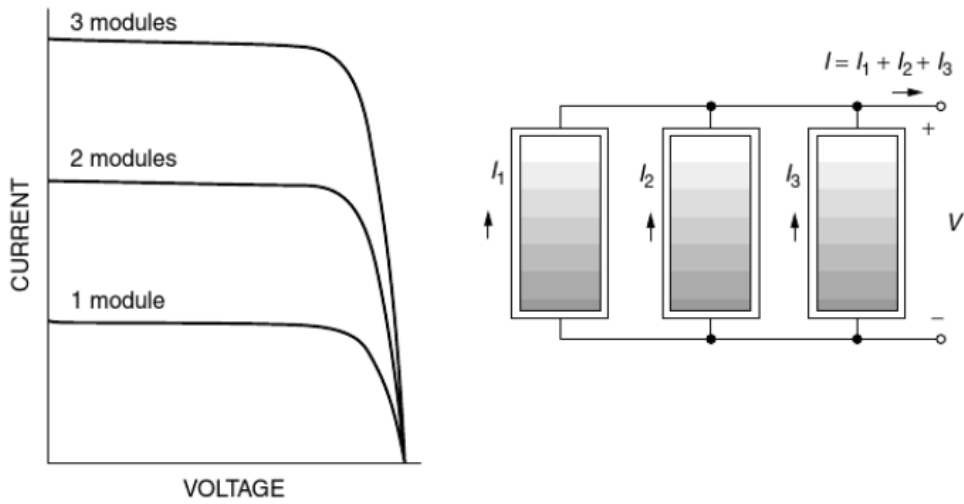
Figure 1.8 : Characteristic current-voltage of Np module in parallel.**[22].**

1.6.3 Blending (series-parallel)

A PVG consists of a series-parallel network of several PV modules grouped by PV panels, **Figure (1.9)**. In order to obtain satisfaction with the present and the time, it is necessary to use mixed groupings, that is to say series and parallel.
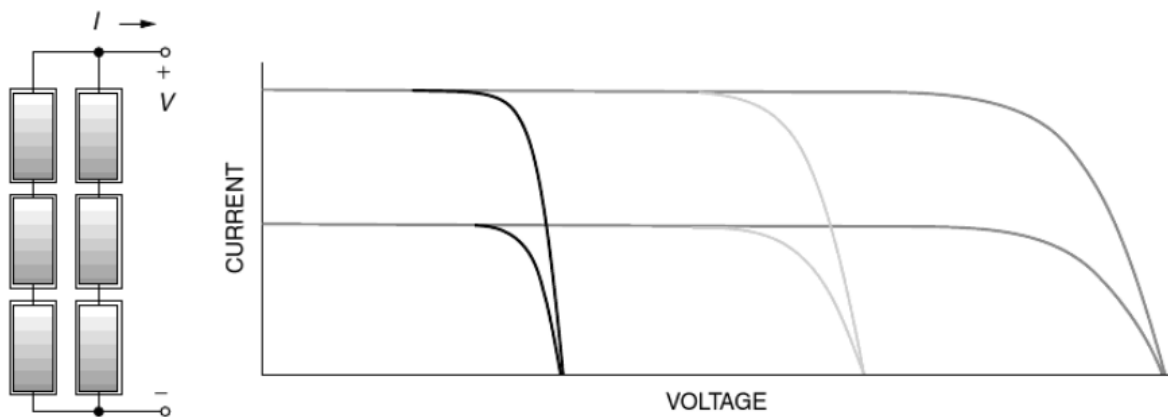
Figure 1.9 : Mixed combination of solar modules **[22].**

1.7 Different types of PV systems

There are generally three PV systems, autonomous systems, hybrid systems and systems connected to the network. The first two types are independent of the electricity distribution system and are often located in remote areas.

1.7.1   Autonomous PV system

Autonomous or «stand-alone», these isolated installations are not connected to the network, the output power of the PVG is not sufficient to satisfy the load demand, also the autonomous PV system is provided by an energy storage system and the latter is used immediately (pumping, ventilation, etc.), and the direct current produced feeds directly to the devices provided for this purpose or is transformed into 230 volts alternative.

This PV system generally includes several basic components:

One or more PV modules

The control system One or more batteries

The UPS.

These systems are generally used in remote and isolated areas of the system.
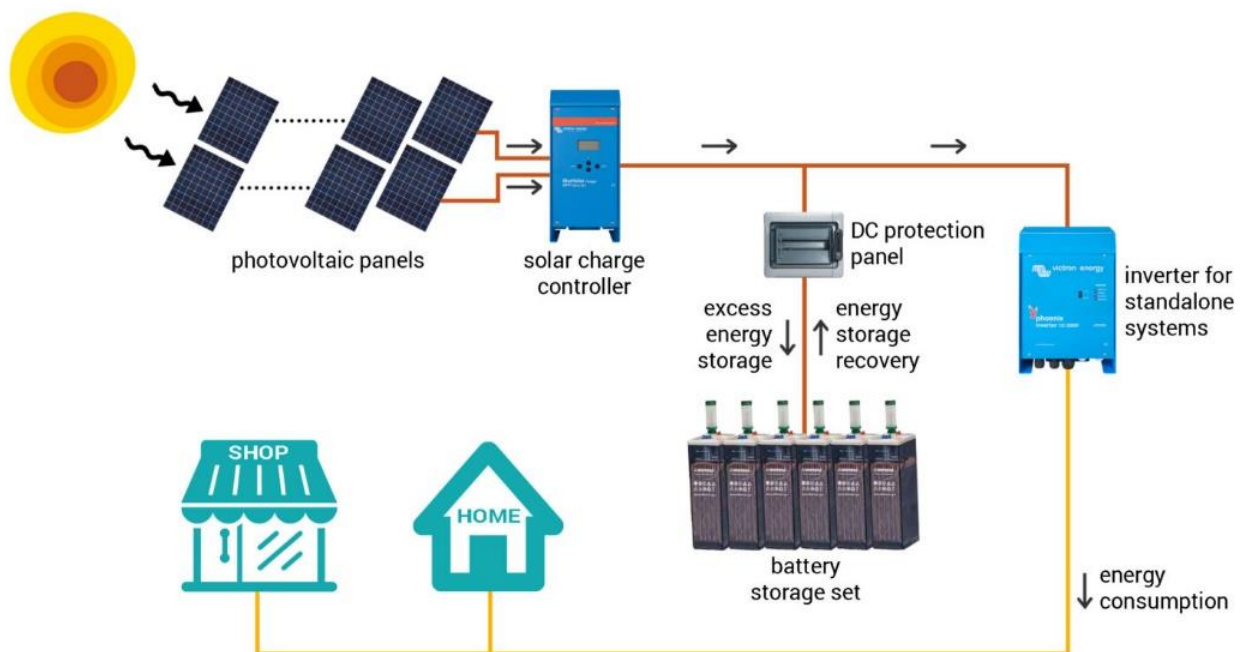
Figure 1.10 : Autonomous PV system.**[23].**

1.7.2 Grid-connected PV system

Not autonomous or grid connected, the system can also be connected to the network, shows a configuration of this system. The advantage of the connection is to dispense with the costly and problematic storage of electricity.

Systems connected to a network reduce the need to increase the capacity of transmission and distribution lines. It produces its own electricity and sends its surplus energy to the grid, from which it supplies itself if necessary, these transfers eliminate the need to buy and maintain a battery. It is always possible to use these systems as backup power when a network failure occurs.
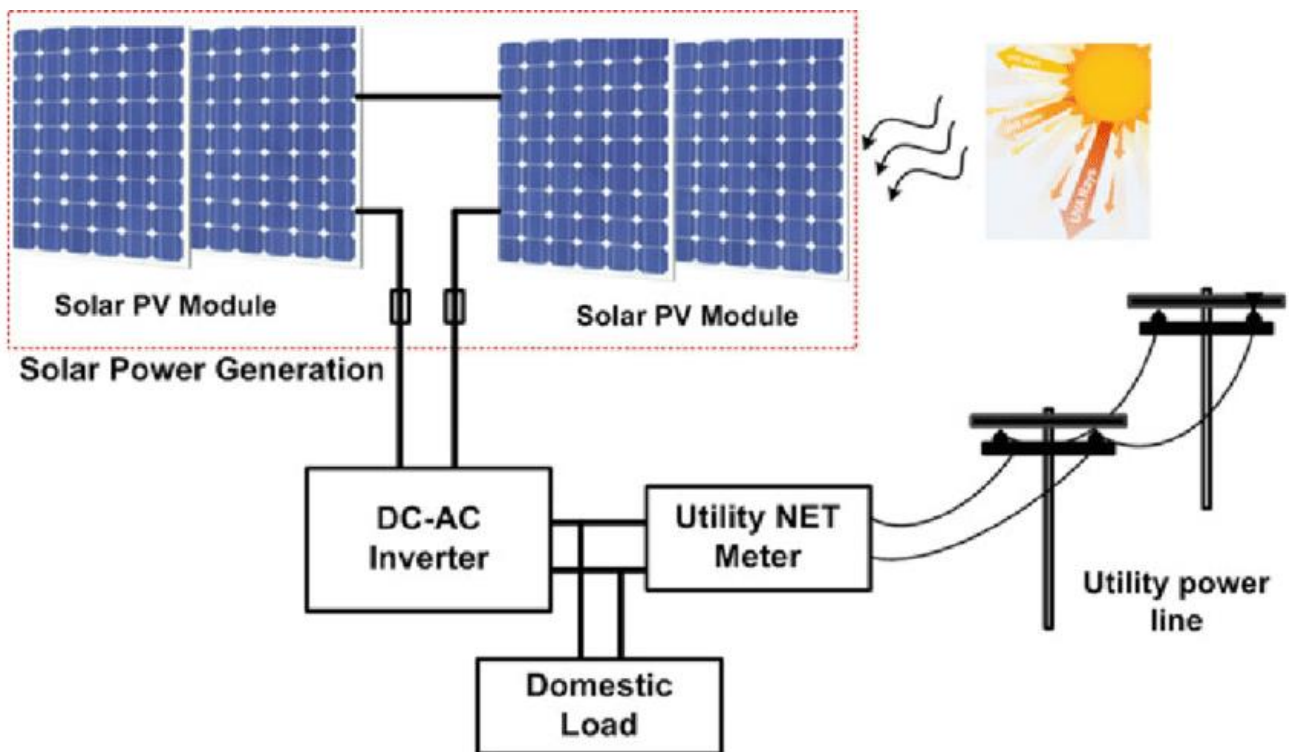
Figure 1.11 : Grid-connected PV installation . **[24].**

1.7.3 Hybrid PV system

Hybrid PV installations integrate a PVG with another: wind turbines, generators, hydroelectric systems... and sometimes even the public network.

Battery systems typically store energy so that energy from random sources such as solar or wind is not lost.

The complexity of such a system lies in the balancing of the different energy sources to optimize them, the sources of heat (diesel, gas, etc.) and public networks being known to always be a last resort.

Hybrid energy systems are often independent of interconnected grids and are often used in isolated areas.

Different sources in a hybrid system can be connected in two configurations, continuous bus architecture and alternative bus architecture.

This type of installation is used when the PVG alone does not cover all the required energy **.**

Figure 1.12 : Hybrid solar system **[25].**

1.8 Advantages and disadvantages of PV energy

1.8.1 Advantages

PV solar panels have a number of advantages:

- This renewable energy is free and independent energy.
- It is not taxed and does not create emissions in the environment throughout its use.
- PV energy is scalable and can meet all needs.
- PV energy is a specific, non-polluting energy that does not generate greenhouse gases or waste.
- Reduces vulnerability to power outages.
- The resale of the production surplus makes it possible to amortize investments and even generate profits.
- Minimal maintenance
- PV panels can be used both in the city and in the countryside.
- The panels are weather and cold resistant.
- The panels have a lifespan of 20 to 35 years.

1.8.2   Disadvantages

Although PV solar panels have many advantages, they also have their disadvantages:

- The actual conversion efficiency of a module is low, around 10-15% with a theoretical limit for a 28% cell PVGs are only competitive with diesel generators for low energy demands in isolated areas **.**
- The production of PV panels is a high-tech sector that requires a lot of research and development and therefore high investment.
- Requires backup system (batteries) for domestic installations.
- In winter, the installation is less efficient. So it must be coupled with additional heating that will do the job.

1.9 Conclusion

In this chapter, we have presented general information on solar energy, the construction of different types of PV cells and their effect as well as their operating principle, and the advantages and disadvantages of PV systems.

Chapter 2   PVG Modeling using Scaps 1-D Software

2.1. Introduction to Numerical modeling

Numerical modeling or analysis is a computer simulation program which uses the mathematical model for the implementation of a physical system. Numerical modeling is the tool to study the system behavior having complex mathematical models and helps provide analytical solutions. It is an essential tool for better understanding of the working parameters of any device. Numerical analysis can play a significant role in the manufacturing and fabrication of efficiently working semiconductors based PV devices. For design engineers and researchers, the highest priority job of numerical modeling techniques implementation is the integration of real-life problem with virtual machine environment because of finding the optimum and efficient ways for solving a complex problem. The precious time is saved due to performing the real design problem in computer-based tests environments without physical or practical implementation, so research institutions and universities emphasize computer-based learnings techniques. Themodeling techniques are used to compute the fundamental physical properties such as holes and electrons concentration and electrical potential. It also provides more information regarding the influence of material physical parameters on device functional parameters or characteristics. For the numerical modeling of solar cells, physical parameters of material are taken as input for the simulation software. To translate the practical or real device $J - V$ characteristics and functional parameters such as power conversion efficiency, fill factor, open circuit voltage and short circuit current in device modeling, it is mandatory to take experimental data. Numerical simulation provides a better and easier way to understand the device behavior. For the better understanding of the performance of a device, the simulation software that can be used for device modelingmust be able to solve semiconductor basic equations like continuity equation for holes andelectrons and the Poisson equation relating the charge to electrostatic potential **[27].**

2.2. Basic semiconductor equation

To analyze the performance of the solar cell, device simulation software must be able to solve the basic semiconductor equations. In device performance, these equations play a crucial role. The Poisson equation relating the charge to electrostatic potential is the governing equation. *Poisson's equation* for electrostatic potential (V) is given in equation II.1 **[26].**

$$\frac{d^2V}{dx^2} = \frac{\rho}{\varepsilon} \qquad (II.1)$$

Where ε is the product of permittivity of free space ε_0 and semiconductor dielectric constant k_s i.e. ($\varepsilon = \varepsilon_0 k_s$) and ρ is the density of charge (C/cm^3) .

From charge neutrality equation ρ can be expressed as given in equation II.2 with an assumption that dopant is totally ionized.

$$\rho = q(p - n + N_D^+ - N_A^-) \qquad (II.2)$$

Where q is electronic charge, p is concentration of holes, n is concentration of electrons, N_A^- ionized acceptor dopant carrier concentration and N_D^+ is ionized donor dopant carrier concentration. By putting equation II.2 in equation II.1 it will become as equation II.3.

$$\frac{d^2V}{dx^2} = \frac{q\ (p - n + N_D^+ - N_A^-)}{\varepsilon} \qquad (II.3)$$

and to solve equation II.3 for V as a function position value of x one must have to rearrange the expression for the concentration of carriers (p, n).

The second equation is a continuity equation, the reason that the continuity equation is called governing equation because drift, diffusion, generation, and recombination are analyzed simultaneously. Equation II.4 and equation II.5 represent continuity equation for concentration change in electron and hole.

$$\frac{\partial n}{\partial t} = -\frac{1}{q}\frac{\partial Jn}{\partial x} + (Gn - Rn) \qquad (II.4)$$

$$\frac{\partial p}{\partial t} = \frac{1}{q}\frac{\partial Jp}{\partial x} + (Gp - Rp) \qquad (II.5)$$

The output from equations II.1, II.4 and II.5 have non-linear dependencies on charge carrier concentration (p, n). Therefore, these equations will be solved with numerical techniques with standard approaches like the discretization of an equation, discretization of device and set of boundary conditions. To measure the current and characteristics of solar cell simulator must be able to solve drift-diffusion equation for current in a solar cell. The *drift-diffusion equation* of charge carriers is given in equation II.6 and equation II.7 .

$$J_n = \epsilon + qD_n \partial n \qquad\qquad (II.6)$$

$$J_p = \epsilon - qD_p \partial p \qquad\qquad (II.7)$$

Jn and Jp are the current densities for electron and holes, μn and μp are mobility of carriers ,D_n and D_p are diffusion coefficient of electrons and holes and from Einstein relationship, the diffusion coefficient is depended upon the mobility of carrier with the product of carrier lifetime. Relation of D_n with the mobility of carrier is given in equation II.8.

$$D(n, p) = \sqrt{\mu}(n, p) \frac{KT}{q} r(n, p) \qquad\qquad (II.8)$$

To find the solution for equations II.3, II.4 and II.5 other quantities needed like generation and recombination (G, R) and this can also be expressed as net recombination in a device (U). That is represented in equation II.9 for n −type semiconductor.

$$U = \frac{p - p_0}{r_P} \qquad\qquad (II.9)$$

2.3. PV device modeling tools

Principally solar cell modeling tool can be capable to solve the basic semiconductor equations such as Poisson equation and continuity equation. To simulate the realistic cells, numerous additional requirements must be met by the device modeling software. They must be able to simulate multiple layers. Simulation tool should be able to give the response and correctly treats the recombination problem and, on an interface, and different layers defects. The modeling software must be able to calculate and simulate the electro- optical measurements under illumination and dark conditions, and this is not only JV characteristics but also the capacitance and spectral response.

To measure and analyze the different solar cell parameters, numerous tools are available and efficiently

used for device modeling. Engineers and researchers are using different types of PV simulation software's in their research centers and in universities **[27].**. Most commonly used software's are enlisted below.

i. $SCAPS-1D$ (Solar Cell Capacitance Simulator)

ii. $AMPS-1D$ (Analysis of Microelectronics and Photonics Structures)

iii. $SILVACO$

iv. $TCAD$

v. $AFORS-HET$ (Automat FOR Simulation of Heterostructures)

vi. $PC1D$

vii. ASA (Amorphous Semiconductor Analysis)

We use $SCAPS-1D$ software for my research work because of the extensively available literature on PV device modeling and analyzing the performance.

2.4. SCAPS 1-D

Solar Cell Capacitance Simulator ($SCAPS$) program developed at the University of Gent,Belgium is used to simulate the PV devices. Several researchers have contributedto its development such as Alex Niemegeers, Marc Burgelman, Koen Decock, Stefaan Degrave, Johan Verschraegen. $SCAPS-1D$ is the one-dimensional simulation program for the modeling of PV devices. Seven different semiconductor layers exclusive of back and front contacts are possible to take as input in $SCAPS-1D$ software. $SCAPS-1D$ tool is freely available for the PV research community and can be freely downloaded from its web link. It runs on a window operating system environment. This software is designed to simulate and helps us to analyze the $J-V$ characteristics curve, accharacteristics ($C-V$ and $C-f$), spectral response (QE) of a device, power conversion efficiency (PCE), fill factor (FF), short-circuit current (J_{sc}), open circuit voltage *(V_{oc})*, energy bands of materials used in solar cell and concentration of different material used by solving the semiconductor basic equations **[28].**

2.4.1. Parameters

For device modeling, input parameters or physical parameters are the fundamental requirements to solve the basic semiconductors equations. The physical parameters used in $SCAPS-1D$ software for numerical analysis are layer thickness, electron-hole mobility, intrinsic carrier concentration, electron

affinity, band gap and doping density ofabsorber, buffer and window layers, which are enlisted in **Table 2.1** . Where N_v is the valence band effective density of state and N_c is the conduction band effective density of states in cm^{-3}. p is the hole concentration and n is electron concentration in cm^{-3}, W is the thickness in μm. χ is the electron affinity in eV, E_g is the bandgap in eV,μe is the electron mobility in cm^2/Vs, μ_p is the hole mobility in cm²/Vs, All the simulations are conducted under $1.5AM$ solar radiation with the power density of 100 mW/cm^2 is used as the illuminating source. Functional parameters of solar cells are given in **Table 2.2** .

The device creation has two common objectives. First is the understanding and verification

of real device behavior and the second one is the simulation of a device for given physicalparameters and predicting the outcomes for those parameters. A good device modeling isdefined by the behavior of the reference device (s) was how much well simulated. For thecreation of device modeling, physical or input parameters are collected form referenced device experimental data. $SCAPS$ offers a single simulation of $J-V$ characteristics curve,ac characteristics $(C-V$ and $C-f)$ and spectral response (QE) and advance batch simulations by varying the input parameters. Predefined physical parameters such as carrier concentration densities and layer thickness are monitor and analyze with the help of batch simulations. J – V characteristics curve, band alignment diagram, spectral responseand other functional parameters such as PCE, FF, J_{sc} and V_{oc} are taken as output from $SCAPS$-$1D$ software, which is very helpful for the fabrication of an efficient PVdevice. All measurements are calculated for illuminated or dark condition and as a functionof temperature. Temperature-dependent parameters are the thermal velocity and effectivedensity of states whereas band gap and mobility are temperature independent parameters. Shockley-Read-Hall (SRH) formalism is used for recombination at the interface states and in deep bulk level and their occupation.

Table 2.1 : Physical parameters for numerical modeling..

No.	Parameters	Abbreviation	Unit
1	**Layer Thickness**	**W**	**μm**
2	**Bandgap energy**	**E_g**	**eV**
3	**Conduction band effective density of states**	**N_c**	**cm^{-3}**
4	**Valence band effective density of states**	**N_v**	**cm^{-3}**
5	**Dielectric permittivity**	**ε_r**	**-**
6	**Electron affinity**	**X**	**eV**

No.	Parameters	Abbreviation	Unit
7	Hole mobility	μ_p	cm^2/Vs
8	Electron mobility	μ_e	cm^2/Vs
9	Electron doping concentration	N	cm^{-3}
10	Hole doping concentration	P	cm^{-3}
11	Absorption coefficient	A	cm^{-1}
12	Bulk defect concentration	N_T	cm^{-3}
13	Capture cross-section	Σ	cm^2
14	Defect energy level	E_T	eV
15	Metal work function	Φ_M	eV

Table 2.2 : Functional parameters..

No.	Parameters	Abbreviation	Unit
1	Power Conversion Efficiency	PCE, η	**%**
2	Short circuit current	J_{sc}	**mA/cm^2**
3	Open circuit voltage	V_{oc}	**v**
4	Fill factor	FF	**%**

2.4.2. SCAPS startup panel interface

SCAPS 1-D simulator, startup panel interface is shown in **figure 2.1**, Several sections of the panel are highlighted by the numbers from 1 to 6.
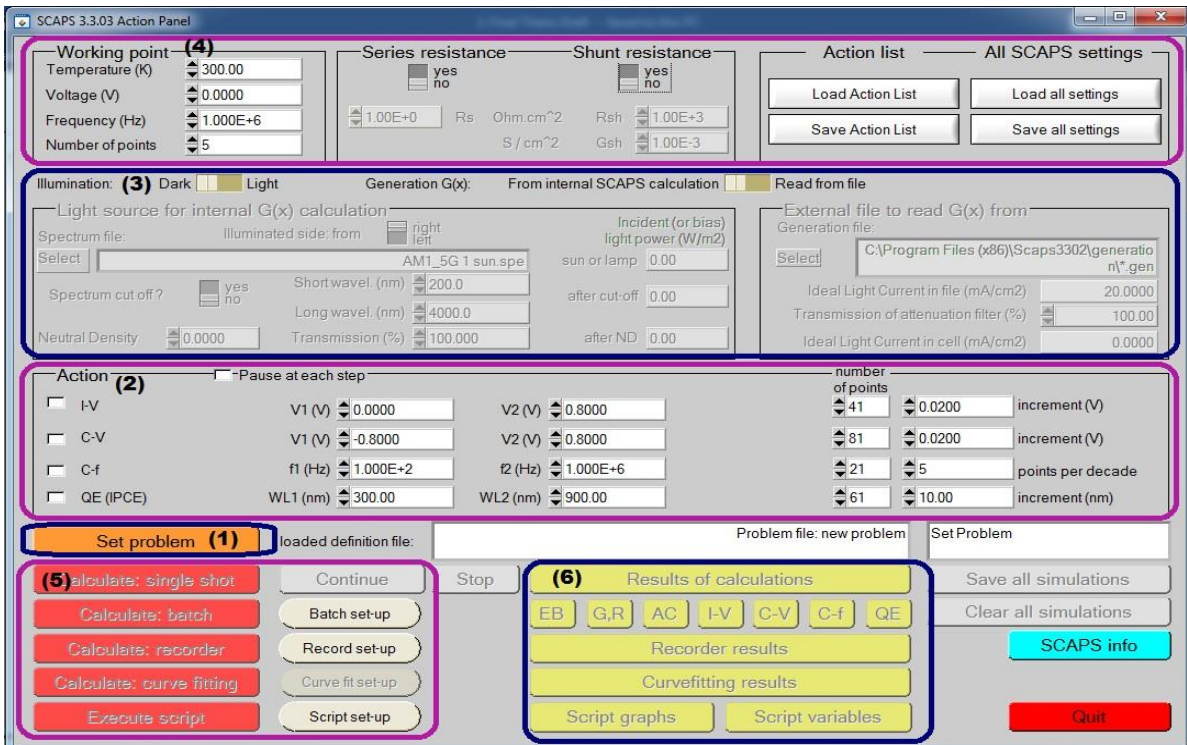
Figure 2.1 : SCAPS − 1D simulator startup panel interface

i. *Section 1* is "Set problem" for the problem definition of the structure of a solarcell. Problem definition mainly having the details about the physical propertiesof different device layers. By clicking on the button "Set problem" another panel is open, where we define different layer physical properties.

ii. *Section 2* is "Action" panel for different measurements of simulations and reading scale settings. This section includes $I − V$ characteristics scale settingsand calibration, Quantum efficiency (QE) measurements, capacitance-voltage ($C − V$) measurements and capacitance frequency ($C − f$) measurements. Startand end values of argument and number of steps are adjusted if required.

iii. *Section 3* is "Illumination" for the selection of light and dark condition for simulation and spectrum standards.

iv. *Section 4* is "Working point" for settings of working temperature values and addition of series or shunt resistances if required.

v. *Section 5* is for single shot calculations, batch calculations and curve fitting fora simulated device. Batch values and their parameters are also selected here.

vi. *Section 6* "Result of calculations" for the measurement and displaying of simulated device results such energy band (EB), $I − V$, QE, $C − V$, and $C − f$ characteristics.

2.4.3. Problem definition interface

Problem definition mainly having the details about the physical properties of different device layers. By clicking on button "Set problem" another interface is open, where we define different layer physical properties. This interface is also named as "Device Definition Interface" and shown in **Figure 2.2**. This interface plays a significant role in device simulation because of defining or setting different layers of physical parameters and device structure visualization.
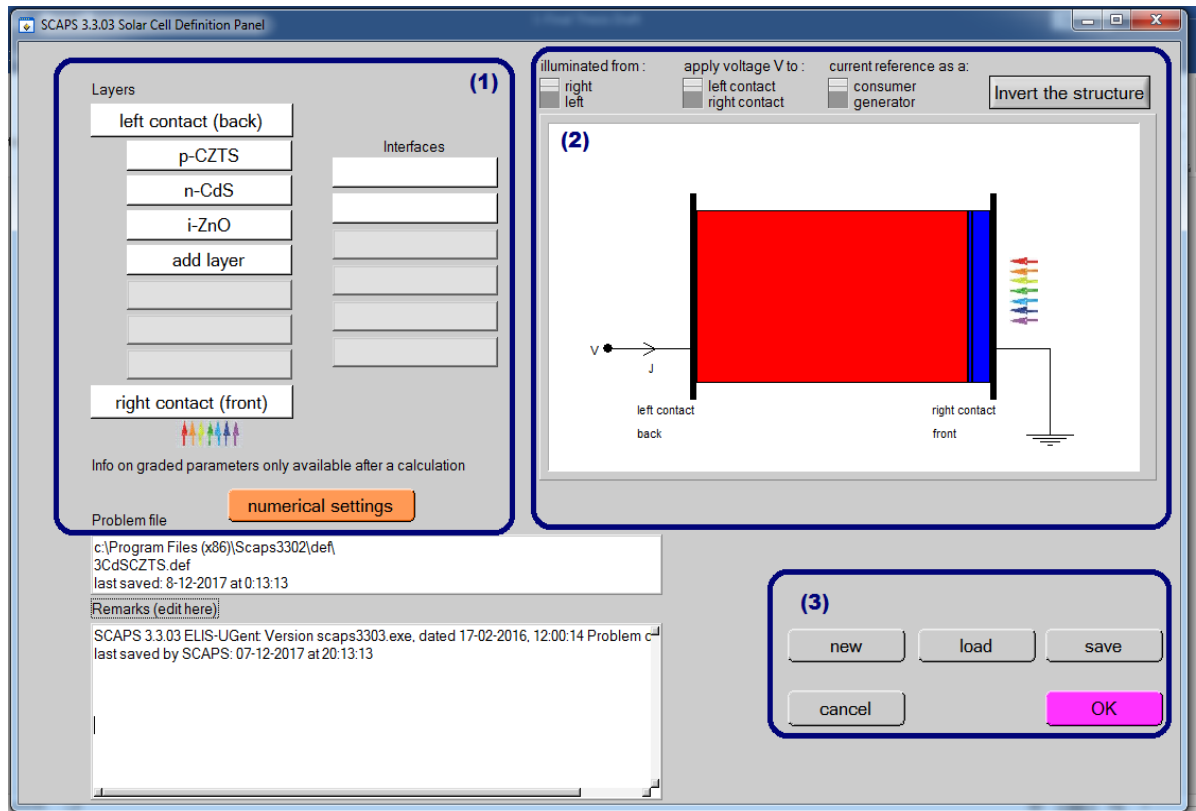
Figure 2.2 : Device definition interface.

There are three parts of device definition interface and details of these sections are as following.

i.   *Section 1* is for the definition of a different layer of device structure with front and back contact. We can simulate a maximum of 7-layers structured device in *SCAPS* software.

ii. *Section 2* is for display or visualization of defined PV device structure with back and front contact. Additional buttons are for the selection of illuminating the device either from back contact side or front contact side, the voltage applied to a device and current reference.

iii. *Section 3* having buttons for saving definition file in *SCAPS* library and loading of device structure definition files. Cancel and OK buttons are for leaving or entering device definition interface and return the user in startup interface.

2.4.4. Adding device structure layers

Adding or defining layers in $SCAPS-1D$ software for modeling of PV device is done byclicking on the button "add layer" given in section 1 of **Figure 2.2**. By clicking the button layer properties interface will be open. We set or add the layer physical parameter values in layer properties interface. The interface is shown in **Figure 2.3**.
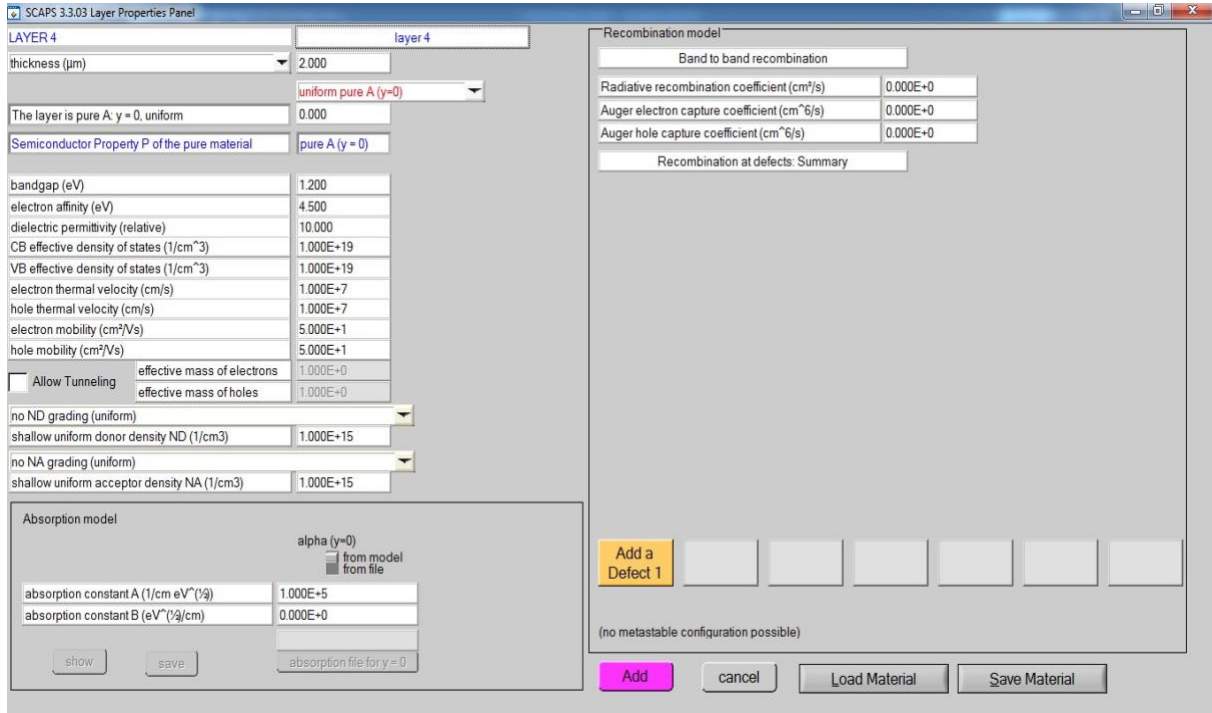
Figure 2.3 : Layer properties panel.

Numerical modeling or analysis of defined device structure is performed in $SCAPS-1$ software after defining physical parameters of all layers such as absorber layer, buffer layer, and the window layer. Effect of different layers physical parameters on the PV device performance are analyzed. These physical parameters are absorber and buffer layer thicknesses, their doping concentrations and operating temperature.

2.5. Numerical modeling of CdTe solar cell

Electrical characteristics of a PV cell are analyzed by simulating the device in *SCAPS* software. Numerical modeling of CdTe/CdS/SnOx solar cell is explained in this section. Different parameters, which affects the device performance are also explained. Band gap energy of CdTe BSF layer is smaller than CdS, so photon absorption in CdTe layer is higher. Overall PV conversion efficiency and open circuit voltage (V_{oc}) of thinfilm *PV* cell increases due to the photon absorption. Results taken from this analysis gives a valuable guideline for the fabrication of CdTe based high-efficiency solar cell. An output of a PV device is highly depended on the parameters such as the concentration of charge carriers, temperature, device thickness and also on optical and electrical properties. The structure CdTe/CdS/SnOx PV cell is shown in **Figure 2.4**. The obligatory physical input parameters for the modeling of CdTe based *PV* device use in the *SCAPS* − 1 simulation environment is presented in **Table 2.3** and **2.4**.
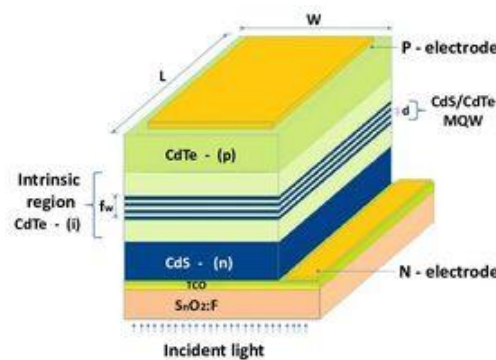
Figure 2.4: Block diagram of CdTe/CdS/SnOx solar cell.**[29]**

Table 2.3 : Simulation parameters for CdTe.

Parameters	p+-CdTe (BSF layer)	n-CdS (Buffer)	p$^+$-SnOx
Thickness, W (μm)	2	0.08	0.5
Bandgap, Eg (eV)	1.50	2.40	3.6
Electron affinity, χ (eV)	3.9	4.0	4.0
Dielectric permittivity, ε_r	9.4	10	9
Effective Density of states, NC (cm^{-3})	8×10^{17}	2.2×10^{18}	2.2×10^{18}
Effective Density of states, NV (cm^{-3})	1.8×10^{19}	1.8×10^{19}	1.8×10^{19}
Electron mobility, μ_e(cm^2/Vs)	320	100	100
Hole mobility, μ_p (cm^2/Vs)	40	25	25
Electron and hole concentration, n, p (cm^{-3})	1.3×10^{14}	3.1×10^{18}	1×10^{17}

Table 2.4 : Interface defects (Neutral) for CdTe.

Defect layer properties	p^+-SnOx	p+-CdTe	n-CdS
Density of defect	1.0×10^{15}cm^{-2}	$2.0\times10^{14}cm^{-2}$	$1.0\times10^{18}cm^{-2}$
Capture cross section area of electrons	$1.0\times10^{-12}cm^2$	$1.0\times10^{-12}cm^2$	$1.0\times10^{-17}cm^2$
Capture cross section area of holes	$1.0\times10^{-15}cm^2$	$1.0\times10^{-15}cm^2$	$1.0\times10^{-12}cm^2$

2.5.1. Energy band diagram of CdTe/CdS/SnOx

Energy band diagram of CdTe/CdS/SnOx structured PV cell is shown in **Figure 2.5**. This energy band diagram was obtained for analysis from the $SCAPS$ software.Energy band diagrams help in explaining the properties of a PV cell.
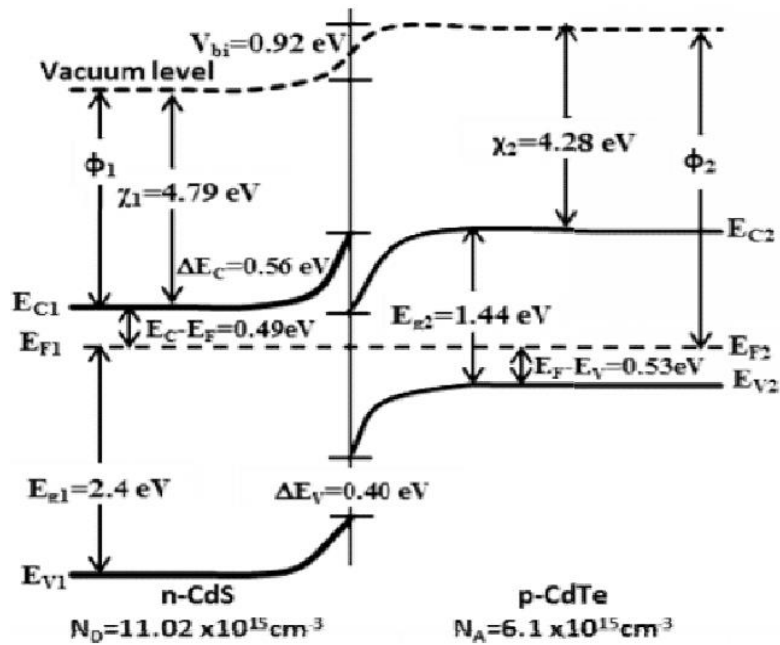
Figure 2.5 : Energy Band diagram of CdTe/CdS/SnOx solar cell ..[30]

2.5.2. $J-V$ characteristics of CdTe/CdS/SnOx solar cell

Figure 2.6 shows the J − V characteristic of CdTe/CdS/SnOx solar cell under illumination.
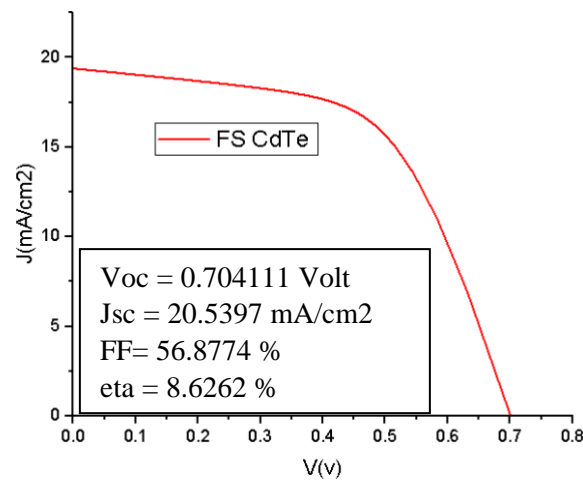
Figure 2.6 : J − V characteristic of CdTe/CdS/SnOx solar cell.

The thickness of CdTe BSF layer taken was 2µm and band gap energy was 1.5eV. Due to incident photons, the PV process starts, these photons will generate charge carriers, which are produced after exposing the cell to sunlight condition of 1 Sun (Air Mass 1.5). Under illumination we see that the CdTe solar cell have a weak efficiency of 8.62% so that means that the PV conversion for a CdTe solar cell is pretty much low comparing to the other solar cell types.

2.6. Numerical modeling of CIGS solar cell
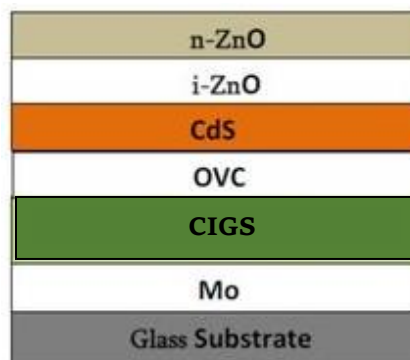
Figure 2.7 : Block diagram of CIGS/OVC/CdS/i-ZnO solar cell . [31]

Table 2.5 : Simulation parameters for CIGS.

Parameters	CIGS	n-CdS (Buffer)	OVC	i-ZnO
Thickness, W (μm)	0.8	0.08	0.015	0.18
Bandgap, Eg (eV)	1.21	2.40	1.45	3.4
Electron affinity, χ (eV)	3.9	4.0	4.5	4.55
Dielectric permittivity, ε_r	10	10	10	10
Effective Density of states, NC (cm^{-3})	2x10^{18}	2.2×10^{18}	2×10^{18}	4×10^{18}
Effective Density of states, NV (cm^{-3})	2×10^{18}	1.8×10^{19}	1.8×10^{19}	9×10^{18}
Electron mobility, μ_e(cm^2/Vs)	50	100	1	50
Hole mobility, μ_p (cm^2/Vs)	20	25	1	20
Electron and hole concentration, n, p (cm^{-3})	5.9×10^{16}	3.1×10^{18}	1×10^{13}	5×10^{17}

Table 2.6 : Interface defects (Neutral) for CIGS.

Defect layer properties	CIGS	OVC	p+OVC/CdS
Density of defect	1.0×10^{18}cm^{-2}	$1.0 \times 10^{17} cm^{-2}$	$1.0 \times 10^{12} cm^{-2}$
Capture cross section area of electrons	$1.0 \times 10^{-15} cm^2$	$1.0 \times 10^{-15} cm^2$	-
Capture cross section area of holes	$1.0 \times 10^{-15} cm^2$	$1.0 \times 10^{-15} cm^2$	-

2.6.1. Energy band diagram of CIGS/OVC/CdS/i-ZnO
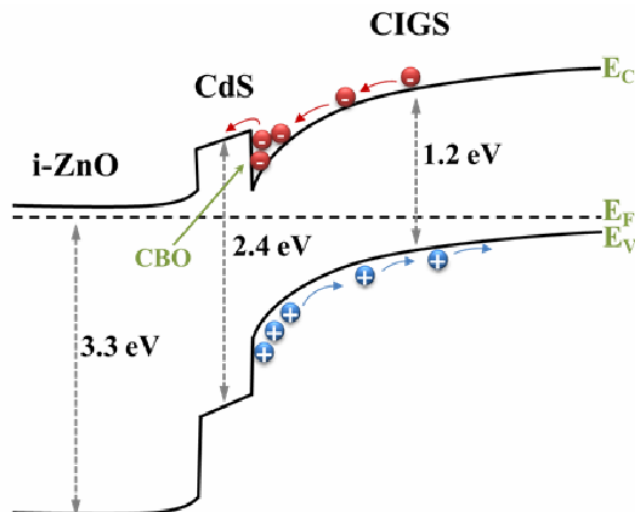
Figure 2.8 : Energy Band diagram of CIGS/OVC/CdS/i-ZnO solar cell .[32]

### 2.6.2. $J - V$ characteristics of CIGS/OVC/CdS/i-ZnO solar cell
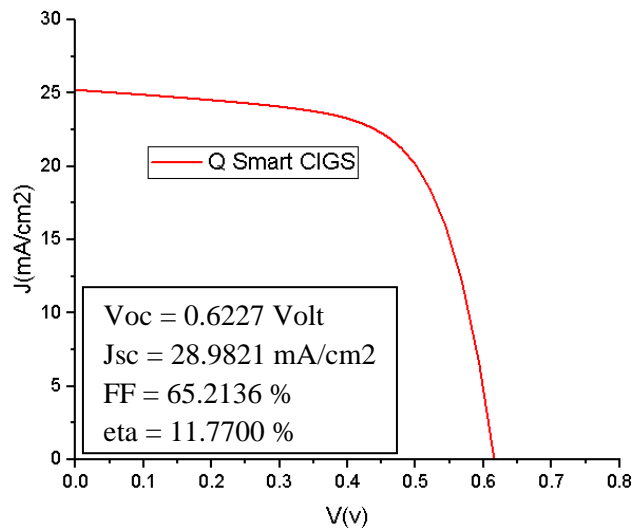
Figure 2.9 : $J - V$ characteristics of CIGS/OVC/CdS/i-ZnO solar cell.

The thickness of CIGS taken was 0.8µm and band gap energy was 1.21eV. Due to incident photons, the PV process starts, these photons will generate charge carriers, which are produced after exposing the cell to sunlight condition of 1 Sun (Air Mass 1.5). Under illumination we see that the CIGS solar cell have a high efficiency of 11.77% so that means that the PV conversion for a CIGS solar cell is higher than the other solar cell types.

2.7. Numerical modeling of Poly-C-Si solar cell
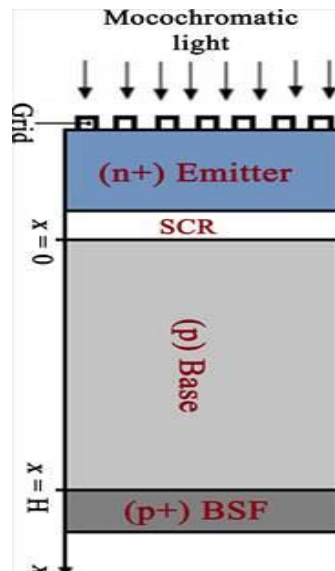
Figure 2.10 : Block diagram of Poly C-Si solar cell . **[33]**

Table 2.7 : Simulation parameters for Poly C-Si..

Parameters	p+ Si (BSF)	p- Si bulk	p- Si front	n-Si
Thickness, W (µm)	2	100	20	0.5
Bandgap, Eg (eV)	1.12	1.12	1.12	1.12
Electron affinity, χ (eV)	4.5	4.5	4.5	4.5
Dielectric permittivity, ε_r	11.9	11.9	11.9	11.9
Effective Density of states, NC (cm^{-3})	2.8x10^{19}	2.8x10^{19}	2.8x10^{19}	2.8x10^{19}
Effective Density of states, NV (cm^{-3})	1.04×10^{19}	1.04×10^{19}	1.04×10^{19}	1.04×10^{19}
Electron mobility, μ_e(cm^2/Vs)	1500	1500	1500	1500
Hole mobility, μ_p (cm^2/Vs)	4500	4500	4500	450
Electron and hole concentration, n, p (cm^{-3})	1×10^{17}	1×10^{17}	1×10^{16}	2.6×10^{16}

Table 2.8 : Interface defects (Neutral) for Poly C-Si.

Defect layer properties	p+ Si (BSF)	p- Si bulk	p- Si front	n-Si
Density of defect	1.0×10^{12}cm^{-2}	1.0×10^{12}cm^{-2}	1.0×10^{12}cm^{-2}	1.0×10^{12}cm^{-2}
Capture cross section area of electrons	1.0×10^{-14} cm^2	1.0×10^{-14} cm^2	1.0×10^{-14} cm^2	1.0×10^{-14} cm^2
Capture cross section area of holes	1.0×10^{-14} cm^2	1.0×10^{-14} cm^2	1.0×10^{-14} cm^2	1.0×10^{-14} cm^2

2.7.1. Energy band diagram of Poly C-Si

Figure 2.11 : Energy Band diagram of Poly C-Si solar cell .[33]

2.7.2. $J - V$ characteristics of Poly C-Si solar cell

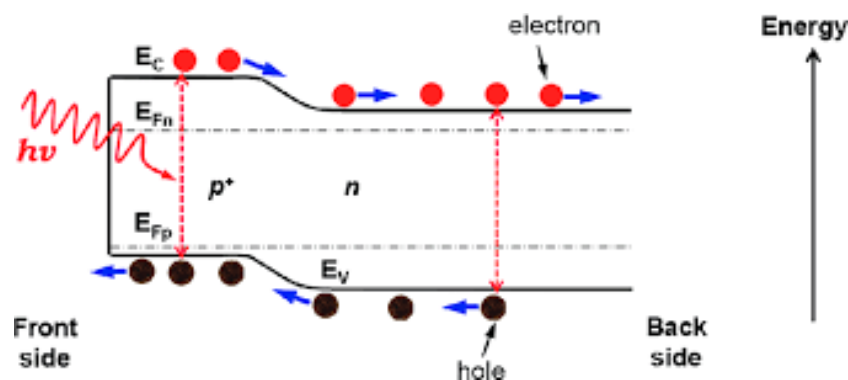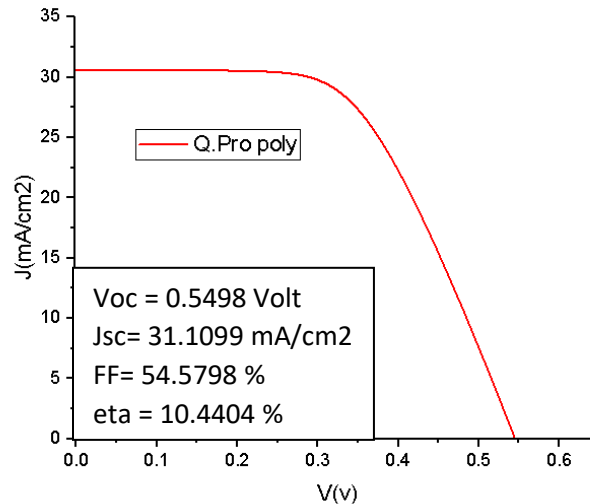**Figure 2.12 :** $J - V$ characteristics of Poly C-Si solar cell.

The thickness of p+ Si BSF layer taken was 2µm and band gap energy was 1.12eV. Due to incident photons, the PV process starts, these photons will generate charge carriers, which are produced after exposing the cell to sunlight condition of 1 Sun (Air Mass 1.5). Under illumination we see that the Poly C-Si solar cell have a medium efficiency of 10.44% so that means that the PV conversion for a Poly C-Si solar cell is satisfying comparing to the other solar cell types.

2.8. Conclusion

Thin film solar cell structure physical operating features are described by different software's. In this work, a detailed analysis of a solar cell was performed on SCAPS-1D software for better understanding of solar cell behavior. In-depth understanding of the solar cell, $J - V$ characteristic measures is not enough to fully describe its behavior, because the behavior or response of a solar cell also depends on its internal physical mechanism. In this work, the performance of a CdTe , CIGS ,Poly C-Si structured PV solar cells was simulated and analyzed on SCAPS simulator software.

Chapter 3 PVG Modeling using Matlab Software (Simscape Model)

3.1 Introduction

Modeling of PVG (which can be solar cell, module, string or array) is central for design, use and control. An accurate model allows (1) predicting the energy yield of PVGs having different configurations of PV modules (e.g., series-parallel, bridge-linked, and total-cross-tied. etc.), (2) evaluating the performance of Maximum Power Point Trackers, (3) performing loss analyses under static and dynamic environmental conditions (e.g., calculating both static and dynamic efficiencies of the whole PV system under different climatic conditions) , (4) analyzing the integration of PV generations to AC and DC distribution systems . Many techniques have been proposed in the literature to model PVGs. For instance, the techniques proposed in are developed for determining the I-V and P-V characteristics. However, those characteristics are not immediately determined as additional steps are required for the computation of several parameters .Sometimes the calculated parameters are sensitive to the climate conditions (e.g., the air humidity) as in . The iterative method presented is sensitive to the initial solution which results in convergence failure. **[34-35-36]**.

Furthermore, even good initial guess cannot ensure convergence. Straight forward methods have the advantage to require less computation and an example of these methods is developed . They are based on an analytical function that depends on the solar cells temperature and the irradiance level to compute current, voltage and power at the Maximum Power Point (MPP). It can be noticed that such methods simplify the computation by avoiding the iterative process but the accuracy is much lowered. Some models ignore the internal resistance to simplify the computation, the obtained results show that accuracy is acceptable. Other techniques have been developed to handle the fact that some PV parameters such as: efficiency, fill factor, open circuit voltage, etc. are climate change dependent. To this, polynomial regression , and Artificial Neural Networks (ANN) have been investigated . Both approaches are typically based on the power rating as input parameter. In addition, the advantage arises from the fact that they can be employed without the need for detailed knowledge about the system under study.

However, the disadvantage of using such approaches is that a large database of climatic and electrical data is needed to be collected in order to model the system. Genetic Algorithm (GA) , Particle Swarm Optimization (PSO) , Differential Evolution (DE) , and Artificial Neural Network (ANN) , etc., have been also employed to find the equivalent circuit parameters. A critical review of various modeling approaches, including analytical models, classical optimization methods and soft computing techniques under different working conditions is

presented . In the other hand, different software are used for the implementation and simulation of PVGs such as, MATLAB, -Maple, Pspice and SABER. **[37-38-39]**

In the light of the previous analysis, one can find that PV model should be at once efficient, accurate and easily to be applied by designers. Moreover, it is much better if the developed PV model uses only the data provided by the manufacture to model any configuration of PV parts (solar cells, bypass diodes, etc). For this purpose, the present work proposes a novel PV model based only on the manufacture's datasheet to model different PV modules having different technologies. Its novelty consists in the usage of a simple procedure to identify the series resistance of solar cells. In addition to the ideality factor value which is adapted to fit the solar cell technology. The proposed PV model uses Matlab-Simscape toolbox (blocks of solar cells, bypass diodes and physical networks) that offers the freedom to modify the configuration of solar cells and bypass diodes by playing on the physical connections between them.

The paper is organized as follows, Section 2 discusses the recent progress and the challenges associated with C-Si and thin film technologies. Section 3 presents the proposed PV model for predicting the I-V and P-V characteristics of different PV module technologies. In section 4, several experimental test results accompanied with several statistical error analyses to validate the proposed PV model are presented. Finally, the paper is ended up with concluding remarks.

3.2 PV modeling using Simscape model

An improved PV model based on Matlab-Simscape toolbox for obtaining the I-V and P-V characteristics is developed. The modeling tools consist of physical-component blocks (i.e., solar cell blocks, bypass diode blocks, etc) and physical-networks. In Simscape environment, Solar cells and bypass diodes can be seamlessly used to model PV modules (i.e., built by interconnecting individual solar cells), PV strings (i.e., built by connecting PV modules in series to get a sufficient voltage) or arrays (i.e., built by connecting PV strings in parallel to get a sufficient current) . Simscape physical networks are employed to connect together any configuration of PV parts as well as to transmit power between them.

The solar cell block provided by Simscape is comprised of a parallel combination of current source, a single diode and parallel resistor (R_p), the latter is connected in series with a resistance Rs. The solar cell current I is given by

$$I = I_{ph} - I_0 \left(\exp\left(\frac{q(V + R_s I)}{KnT} \right) - 1 \right) - \frac{(V + R_s I)}{R_p} \tag{1}$$

Where, V and I represent the solar cell output voltage and current, respectively. Rs is the series resistance of a single solar cell, which has usually a small value representing the contact resistance. However, the parallel resistance Rp possesses a very large resistance that models the leakage current of the P-N junction. q [C] is the charge of an electron (1.602×10^{-19}). I_{ph} is the light current, I_0 is the saturation current, n is the diode ideality factor, K [J/K] the Boltzmann's constant (1.38×10^{-23}) and T is the cell temperature. So, to characterize a solar cell block, the block-parameters solar-cell requires both climatic and electrical parameters. The climatic parameters which are the temperature [°C] and the irradiance [W/m^2], can be obtained by measuring them with the appropriate sensors. The electrical parameters are; the open circuit voltage (V_{OC}), the short circuit current (I_{SC}), the ideality factor n and the series resistance Rs. The Voc and Isc values are obtained from PV module's datasheet. However, n and Rs are not provided.

Previous works to obtain the series resistance by using trial and error method (Orioli et al., 2013, Luque,2011). However, to model a PV plant with different parameters of PV modules, it is a difficult task to find an accurate Rs for each module. In (Walker, 2001), Rs is determined by evaluating the derivative of the model equation at V_{OC} point, which leads to significant computation efforts. An iterative algorithm is used in (Xiao et al., 2004) that is based on the minimization of (dP /dV_{MPP}=0) to find an optimal value of the adjustment factor (α). Once this latter is reached, the Rs can be calculated. Another approach based on optimization is presented in (Ulapane et al., 2011) where the determination of Rs value is carried out by evaluating an expression based on unknown factor and the parameters reported in the datasheet. However, this approach is very sensitive to initial solution as it uses the Newton-Raphson method to determine an unknown factor within the expression of Rs. In the same context, the authors in (Chenni, et al., 2007) has employed a binomial search routine to seek the optimal value of Rs within an estimated interval. However, the use of this optimization method made the determination of Rs a complex task. A complicated function of series resistance is solved iterativelyby using a typical series resistance of the PV module as a starting point. However, the model needs additional information besides the standard data provided by the manufacturer's datasheet. Considering the aforementioned drawbacks, designers of PV systems often find difficulties in applying such models. On the other hand, in many modeling techniques, the ideality factor is not adapted to fit the modeled PV technology. Therefore, it is taken as a random value from the range 1<A< 2.

In the following, a contribution for rendering the Simscape-based-PV model based only one the Manufacture's datasheet is made. Therefore, for each technology of PV modules, a specific ideality factor value is used. Poly C-Si, CdTe and CIGS ideality factors are given in Table 3.1. Moreover, an expression uses the available information in the manufacturer's datasheet to forwardly calculate the value of series resistance Rs has been adopted.

Table 3-1 : Ideality factor for different PV technologies.

Technology	Ideality factor
Poly C-Si	1.3
CdTe	1.5
CIGS	1.5

The Rs calculation is based on the computation of the fill factor which is determined as follows:

$$V_{\_MPP}[p.u] = \frac{V_{MPP}}{V_{oc}} \qquad (2)$$

$$I_{\_MPP}[p.u] = \frac{I_{MPP}}{I_{sc}} \qquad (3)$$

$$FF[\;] = V_{\_MPP}[p.u] \cdot I_{\_MPP}[p.u] \qquad (4)$$

Where, Voc 9V] and Isc [A] are the open circuit voltage and the short circuit current, respectively. FF [ ] is the PV module's fill factor at STC.

The solar cell's series resistance Rs [Ω] (Massi pavan et al., 2014), is calculated as;

$$R_S = \frac{V_{OC}}{I_{SC}} \cdot R_{SN} \qquad (5)$$

R_{SN} [ ] is the normalized solar cell's series resistance that is determined as shown below (Markat, Castañer, 2006)

$$R_{SN} = 1 - \frac{FF}{FF_{N,25}} \qquad (6)$$

Where, $FF_{N,25}$ [ ] is the normalized fill factor when the solar cell temperature is 25° C and given as .

$$FF_{N,25} = \frac{v_{OCN,25} - \ln(v_{OCN,25} - 0.72)}{v_{OCN,25} + 1} \qquad (7)$$

Where, $v_{OCN,25}$ [ ] is the normalized open-circuit voltage at temperature of 25 °C which is calculated as (Massi Pavan et al., 2014);

$$v_{OCN,25} = \frac{V_{OC}}{Vt_{,25}.N_S} \tag{8}$$

Where, $V_{t,25}$ [V] is the junction thermal voltage of the solar cell at 25° C, Ns [ ] is the number cells of the PV module,

Finally, the junction thermal voltage of the solar cell at 25° C is given by;

$$Vt_{,25} = \frac{k.(25+273)}{q} \tag{9}$$

Where, k [J.K^{-1}] and q [C] are the Boltzmann's constant and the electron charge, respectively. Figure 3.1 (a) shows the Simscape implementation of the PV module 'Q.Pro 230Wp' as an example connected to a system for sweeping-acquiring the I-V and P-V characteristics, its main part are:
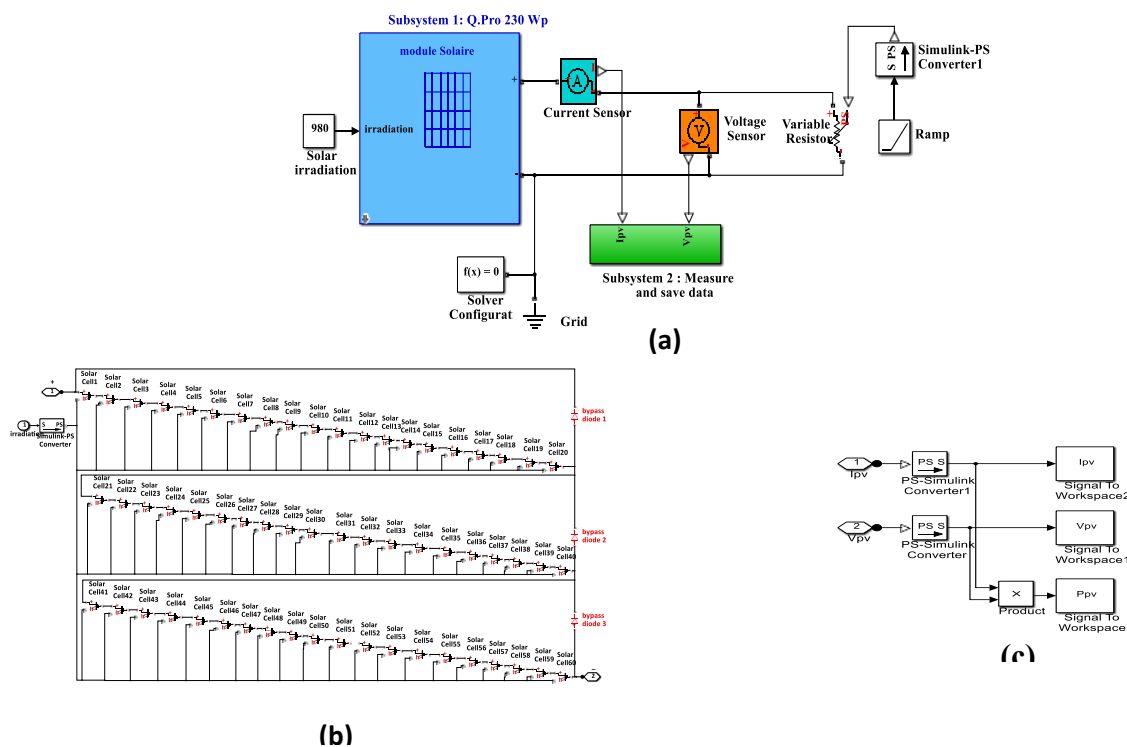

(a)

(b)

(c)

Figure 3-1:Simscape implementation of: (a) 'Q.Pro 230Wp' PV module (b) PV system (c) integrated blocks in subsystem 2..

Subsystem 1: contains the implemented Q.Pro 230Wp PV module illustrated in Fig. 3.1.(b), it is composed of 60 solar cells connected together by physical networks. Each solar cell has been characterized according to the electrical characteristics reported in Table 3.2 as well as the ideality factor values reported in Table 3.1. Eqs (2–9) have been used to compute the solar cell's series resistance.

- **A variable resistor and ramp block**: used to sweep the I-V and P-V characteristics.

- **Current and voltage sensors**: employed to measure I and V, respectively. The measured I and V are acquired and saved by Subsystem 2.
- **Subsystem 2:** used to acquire and save the measured data. Its main blocks are shown in Fig. 3.1 (c).
- **Solver-Configuration-block:** used to determine the unknown variables for the entire modeled system, it can be connected anywhere on the physical network circuit by creating a branching point. It is imperative to fine-tune the solver parameters before running the simulation in order to avoid warning or error message. The solver parameters are chosen as follows: the step-type is *fixed step*, the solver-type is ***Runge-Kutta*** and fixed step size is 0.001.
-

3.3 Data Analysis

A number of measurements have been carried out at the test facility of Triest University, Italy. To this, the three PV modules namely Q.Pro 230Wp (Poly C-Si technology), Q.Smart 95Wp (CIGS technology) and First Solar FS-272 (CdTe technology) have been considered. The electrical specifications of these modules are reported in Table 3.2. Different experiments are conducted at different working condition for each of the above modules. The I-V characteristic of each PV module is recorded by sweeping the output voltage from zero to V_{oc}.

The test facility is shown in Fig. 3.2, where three PV modules are made available. It comprises also two data loggers (type E-Log, MW8024-02/10 produced by LSI Lastem S.r.l) for climatic and electrical data, they are connected to a computer for the data to be collected and saved. DC-DC converter (type Solar Magic produced by National Semiconductor Ltd) connected to a resistive load. One ISO9060 first class thermopile global radiometer type C100R DPA153 (produced by LSI Lastem S.r.l) installed on the same frame carrying PV modules (the daily uncertainty for this device is less than 5%, the sensitivity is 30÷45 µV/(W/m²) and the flat spectral response range is (305-2800 nm)). Three module temperature contact probes (type DLE 124 by LSI Lastem S.r.l) having an accuracy of ±0.15 °C. Three shunts type SHP300A60-Compact (produced by Hobut Ltd) calibrated with an accuracy better than 0.01%. Fast measurements of the I-V characteristics are carried out by varying the duty cycle of the DC-DC converter from the minimum to its maximum value. At this time, both the climatic (irradiance and temperature) and electrical data (PV current and voltage) are simultaneously acquired and stored in the computer.

Table 3.2 : Electrical characteristics of the used PV modules.

Designation	First Solar FS-272	Q.Pro 230Wp	Q.Smart 95Wp
Maximum power (P_{MPP}) [W]	72.5	230	95
Voltage at P_{max}(V_{MPP}) [V]	66.6	29.24	62.1
Current at P_{max} (I_{MPP}) [A]	1.09	7.95	1.53
Open circuit voltage (V_{OC}) [V]	88.7	36.95	78
Short circuit current (I_{SC}) [A]	1.23	8.59	1.68
Cells number N_S	116 cells	60 cells	116 cells
Bypass diodes number	None	3	1
Technology	CdTe	Poly C-Si	CIGS
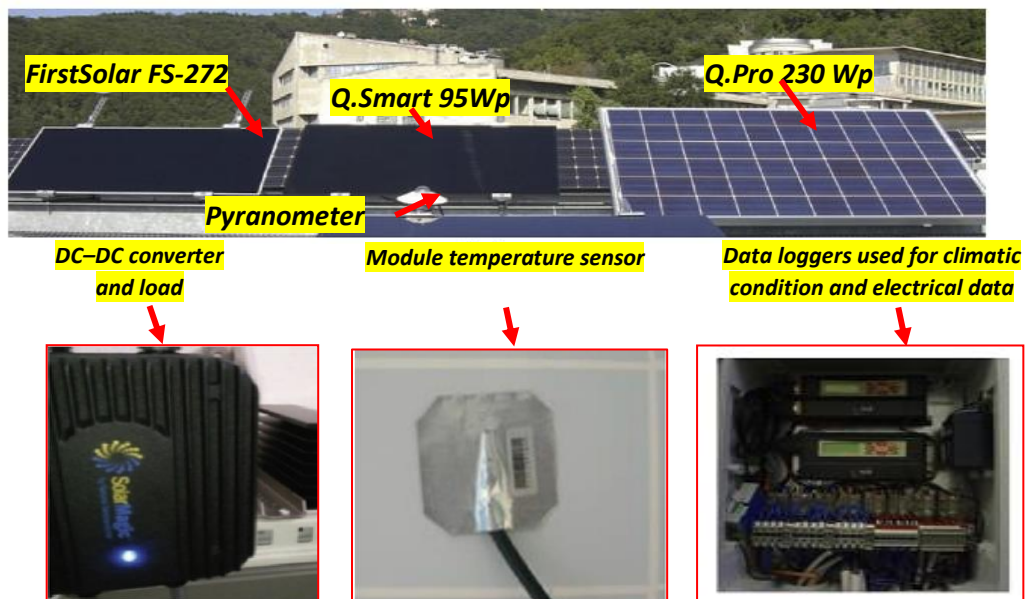
Figure 3.2 : Test facility to measure the electrical characteristics of the used PV modules.
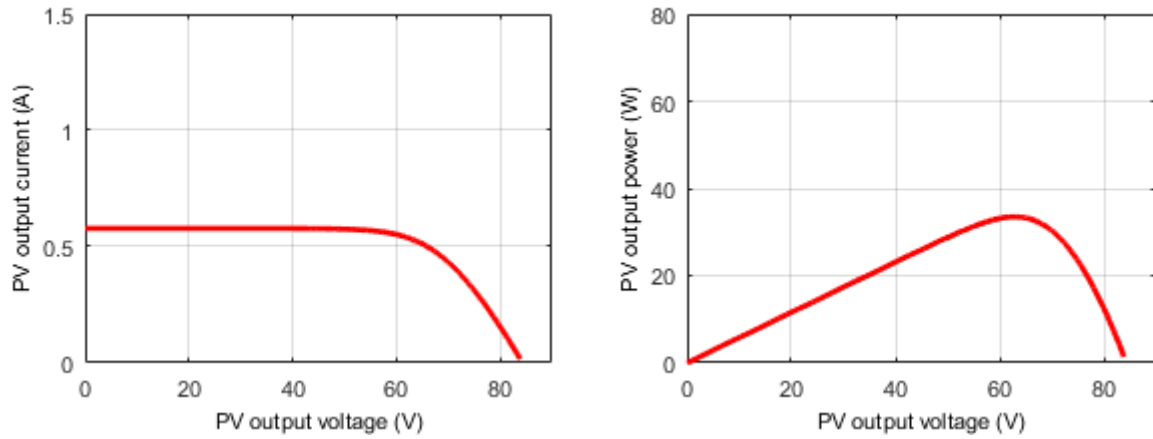
Simulation Results for First Solar FS-272 :

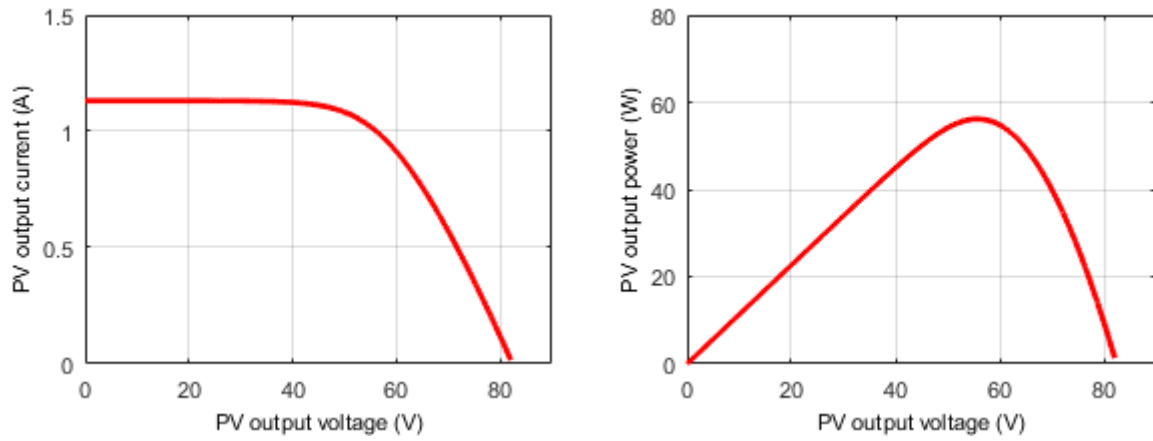**Figure 3.3 :**I-V and P-V characteristics for FS-272 (920 W/m2 ; 56°c).

Figure 3.4 :I-V and P-V characteristics for FS-272 (470 W/m2 ; 30°c)

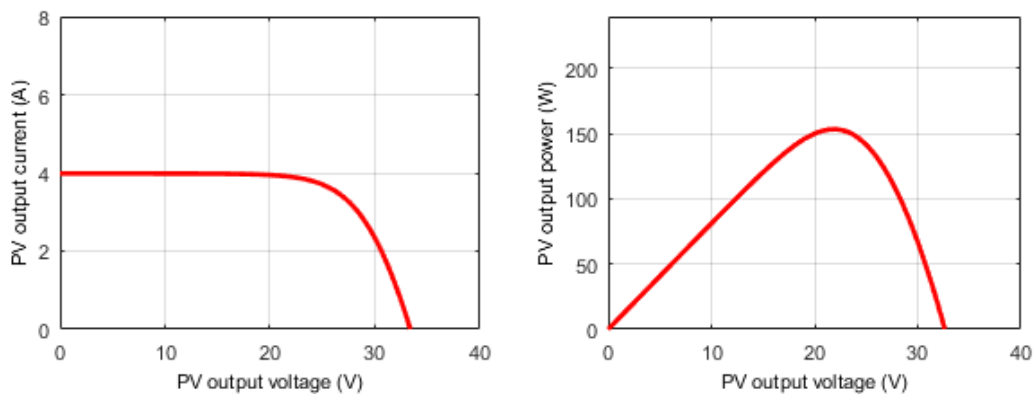**Simulation Results for Q.Pro 230:**

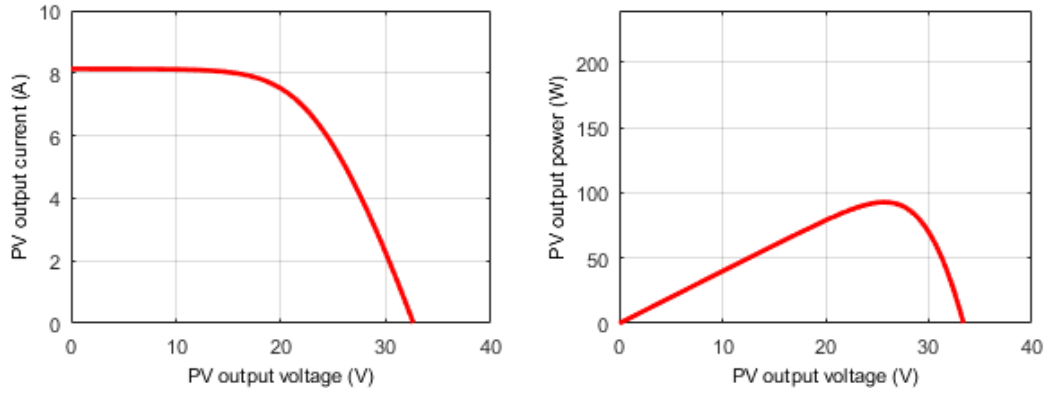**Figure 3.5 :**I-V and P-V characteristics for Q.Pro 230Wp (980 W/m2 ; 55.5°c)

Figure 3.6 :I-V and P-V characteristics for Q.Pro 230 Wp (470 W/m2 ; 30°c)
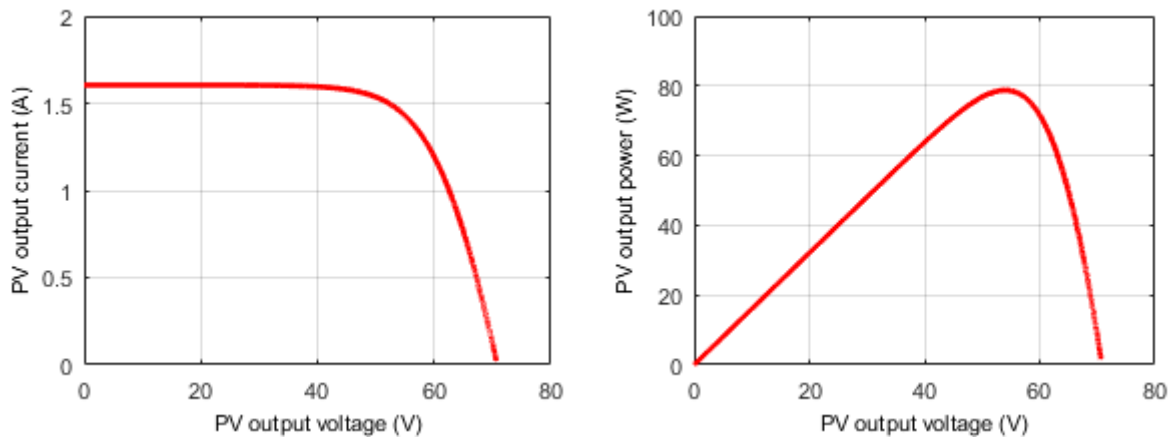
Simulation Results for Q.Smart 95:

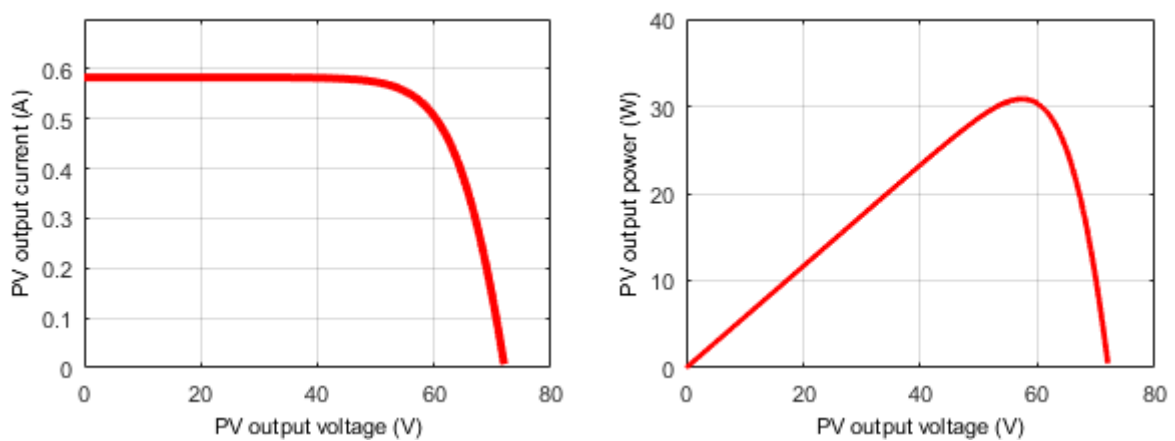**Figure 3.7 :**I-V and P-V characteristics for Q.Smart 95Wp(995 W/m2 ; 56°c)

Figure 3.8 :I-V and P-V characteristics for Q.Smart 95 Wp (347 W/m2 ; 30°c)

.

51

3.4 Conclusion

Modeling a PV module using Simscape toolbox provides several benefits. Simscape offers a versatile platform for accurately capturing the electrical and thermal characteristics of the module. It allows simultaneous consideration of both aspects, enabling realistic representation of module behavior. The graphical interface simplifies model creation and visualization, while integration with other MATLAB/Simulink tools enhances analysis and optimization capabilities. In this work, the performance of a CdTe , CIGS ,Poly C-Si structured PV solar cells was simulated and analyzed.

Chapter 4 Experimental Validation

4.1 Experimental validation of Simscape-based-PV model

The validation of the Simscape-based PV model is carried out to show its effectiveness in predicting the I-V and P-V characteristics for different PV technologies (i.e., Poly C-Si, CdTe and CIGS). Therefore, First Solar FS-272, Q.Pro 230Wp and Q.Smart 95Wp modules are implemented according to the electrical characteristics reported in Table 3.2 as well as the ideality factor values reported in Table 3.1. Simulation is done using the recorded climate conditions. The obtained I-V and P-V characteristics of Simscape-based-PV model have been compared to those measured for the same weather conditions.

The results have been simulated according to the DataSheet Parameters in Table 4.1

Table 4-1: DataSheet Parameters..

Module	Voc (V)	Isc (A)	FF (%)	Vmpp	Impp	eta_calcul (%)	Area (m2)	N_cells	Area_Cell (cm2)	Voc_cell	Jsc_cell (mA/cm^2)
FS-272 CdS/CdTe	88.7	1.23	66.54	66.6	1.09	10.08	0.72	116	62.068	0.764	19.81
Q-PRO230	36.95	8.59	73.24	29.24	7.95	14.22	1.63	60	272.26	0.615	31.54
Q-Smart 75CIGS	74.4	1.66	60	53.6	1.4	9.89	0.75	116	65.386	0.641	25.38

Fig. 4.1 to Fig. 4.6 show the simulated versus the measured data of the I-V and P-V characteristics for each PV technology. It can be noticed that there is a good agreement between the simulated and the measured electrical characteristics.
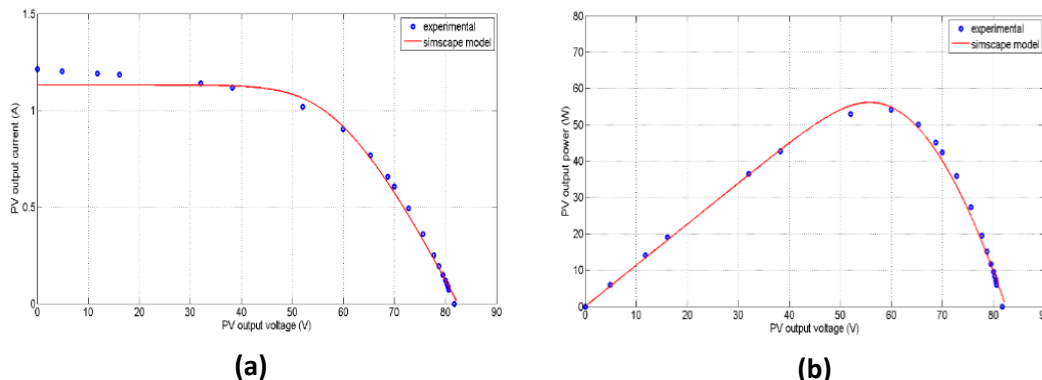

(a)   (b)

Figure 4-1: Experimental data (dotted line), Simscape-model (solid line) for PV module FS-272 operating at G=920 W/m2 and T=56 °C (a) I-V characteristic (b) P-V characteristic.

(a)

(b)

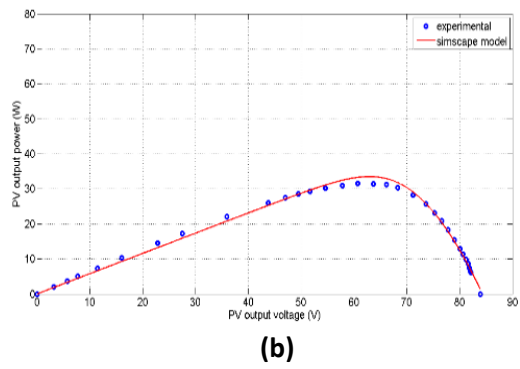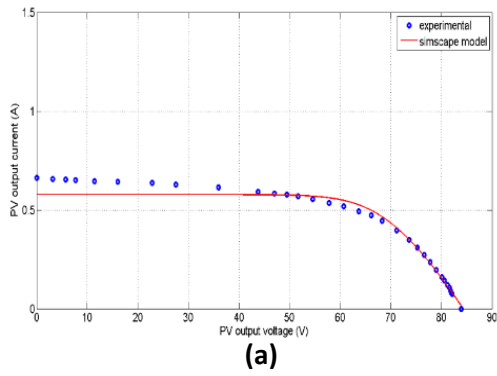**Figure 4-2:** Experimental data (dotted line), Simscape-model (solid line) for PV module FS-272 operating at G=470 W/m2 and T=30 °C (a) I-V characteristic (b) P-V characteristic.

(a)

(b)

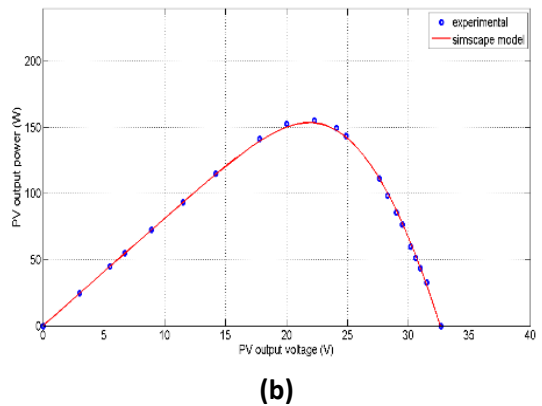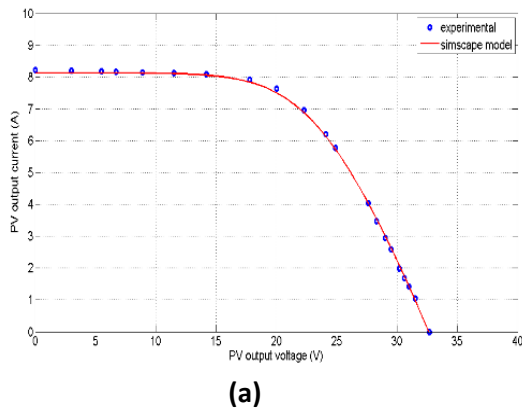**Figure 4-3:** Experimental data (dotted line), Simscape-model (solid line) for PV module Qpro operating at G=980 W/m2 and T=55.5 °C (a) I-V characteristic (b) P-V characteristic.

(a)

(b)

Figure 4-4: Experimental data (dotted blue line), Simscape-model (solid red line) for PV module Qpro operating at G=480 W/m2 and T=36.5 °C (a) I-V characteristic (b) P-V characteristic.

(a) **(b)**

Figure 4-5:Experimental data (dotted blue line), Simscape-model (solid red line) for PV module
Qsmart operating at G=995 W/m2 and T=56 °C (a) I-V characteristic (b) P-V characteristic.
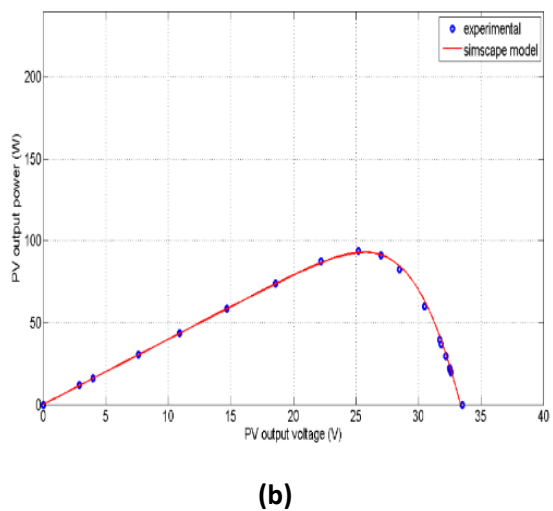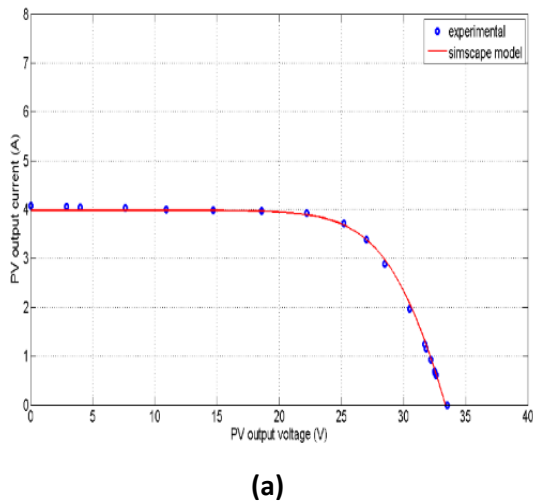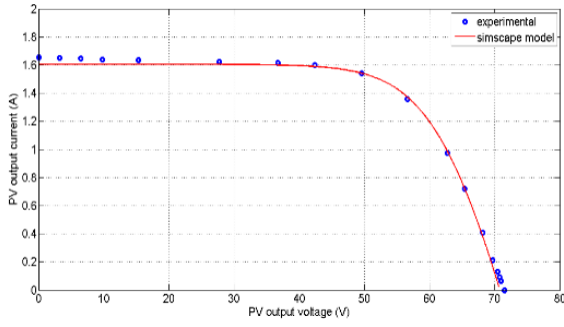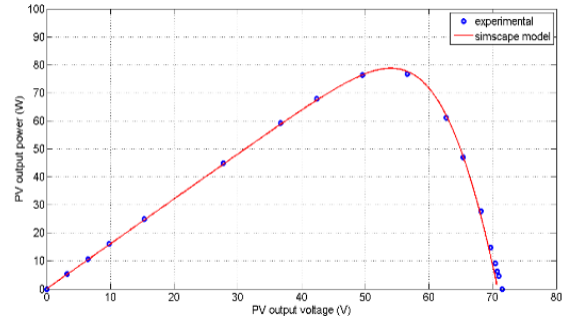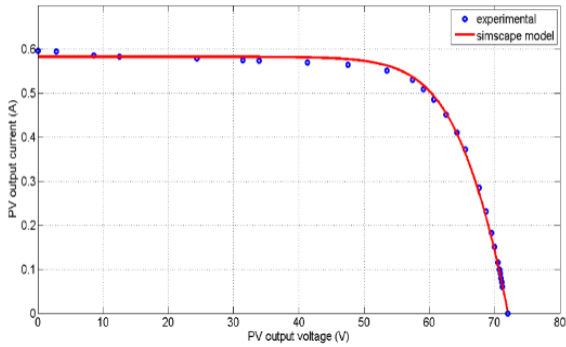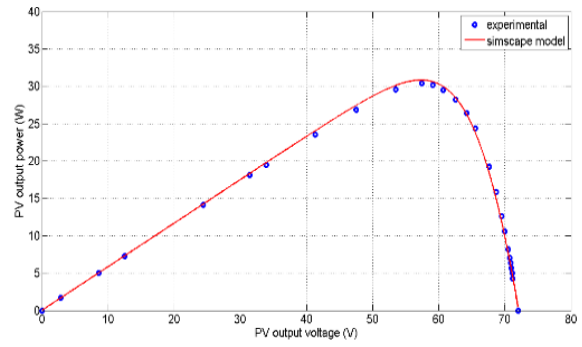

(a) **(b)**

Figure 4-6: Experimental data (dotted blue line), Simscape-model (solid red line) for PV module
Qsmart operating at G=347 W/m2 and T=30 °C (a) I-V characteristic (b) P-V characteristic.

In order to measure the accuracy of the developed Simscape-based-PV model in predicting the
P-V and I-V characteristics of each technology under the considered climatic conditions,
several statistical error tests are used to characterize the degree of matching between the
simulated and the measured characteristics. These statistical error tests are given by the
following expressions:

The root mean square error (RMSE)

$$RMSE[W] = \sqrt{\frac{1}{N} \sum_{k=1}^{N} \left(P_{pv\_mea}(k) - P_{pv\_sim}(k) \right)^2} \qquad (10)$$

56

The correlation coefficient (R^2)

$$R^2[\%] = \left[1 - \frac{\sum\limits_{k=1}^{N}\left(P_{pv\_mea}(k) - P_{pv\_sim}(k)\right)^2}{\sum\limits_{k=1}^{N}\left(P_{pv\_mea}(k)\right)^2} \right].100 \qquad (11)$$

The mean percentage error (MPE)

$$MPE[\%] = \frac{1}{N}\sum\limits_{k=1}^{N}\left(\frac{P_{pv\_sim}(k) - P_{pv\_mea}(k)}{P_{pv\_mea}(k)}\right).100 \qquad (12)$$

The deviation from the measured values (Dev)

$$Dev[\ ] = \frac{\sum\limits_{k=1}^{N}P_{pv\_sim}(k) - \sum\limits_{k=1}^{N}P_{pv\_mea}(k)}{\sum\limits_{k=1}^{N}P_{pv\_mea}(k)} \qquad (13)$$

Where $P_{pv\_mea}(k)$ [W] is the *kth* measured value of the PV output power, $P_{pv\_sim}(k)$ [W] is the *kth* simulated value of the PV output power and N [ ] is the number of simulated or measured points.

Table 4-2: Comparisons between simulated and measured P-V curves of each used PV technologies for Simscape model.

PV module	technology	G [W/m²]	T [°C]	RMSE [W]	R^2[%]	MPE [%]	Dev [ ]
First Solar FS-272	CdTe	920	56	1.2462	99.82	-0.057	-0.0125
		470	30	0.7937	99.85	0.0357	0.0118
Q.Pro 230Wp	Poly C-Si	980	55.5	0.5976	99.99	0.0031	0.00064
		480	36.5	0.5762	99.99	0.0236	0.0045
Q.Smart 95Wp	CIGS	995	56	0.5767	99.98	-0.0123	-0.0022
		347	30	0.3118	99.97	0.0185	0.0050

Table 4.2 shows, for each PV module and for a given climate conditions, the computed statistical errors. One can notice that the RMSE values are relatively low; ranging between 0.311W and 1.246W. Furthermore, the deviations from the measured values are the range that is [-0.0125, 0.0118]. The correlation coefficient values are greater than 99.8 % regardless the technology of the module and the weather conditions. Moreover, the absolute values of the MPE are always less or equal to 0.057 %. Upon the analysis of these results, it can be concluded

that the proposed Simscape-based-PV model offers a good performance in predicting the electrical characteristics (i.e., current, voltage, power) of different PV technologies, particularly, a PV module having Poly C-Si technology. The latter has the highest correlation values (99.99%) and the lowest $|MPE|$ and $|Dev|$, 0.0031 and 0.00064, respectively. Likewise, the obtained static errors of CIGS PV module lead to say that Simscape-based-PV model can offer satisfactory prediction for this technology. However, the predicted electrical characteristics of CdTe PV module present the poorest performances compared to the remaining. This has the lowest correlation (99.82%) and the highest $|MPE|$ and $|Dev|$ (0.057 and 0.0125, respectively).

Fig. 4.7 to Fig. 4.9 show the simulated versus the measured data of the I-V and P-V characteristics for each PV technology. It can be noticed that there is a good agreement between the simulated and the measured electrical characteristics.

4.2 Experimental validation of SCAPS 1-D based-PV model :
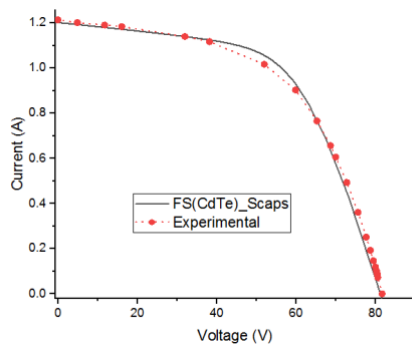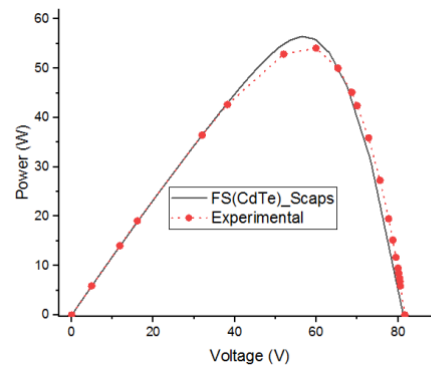
Figure 4-7: Experimental data (dotted red line), SCAPS-model (solid black line) for PV module FS-272 operating at G=1000 W/m2 T=25 °C (a) I-V characteristic (b) P-V characteristic.

Figure 4.8 : Experimental data (dotted red line), SCAPS-model (solid black line) for PV module Qsmart operating at G=1000 W/m2 and T=25 °C (a) I-V characteristic (b) P-V characteristic..

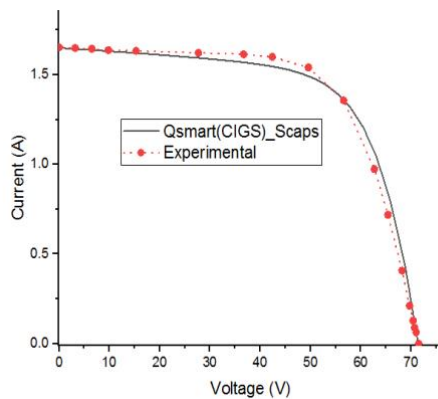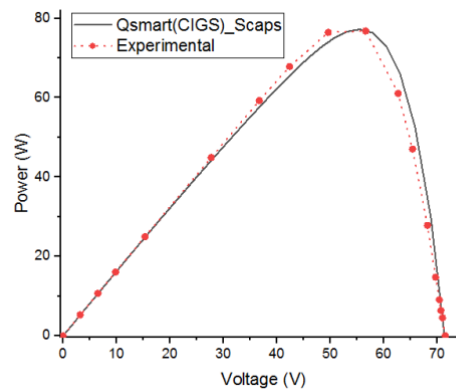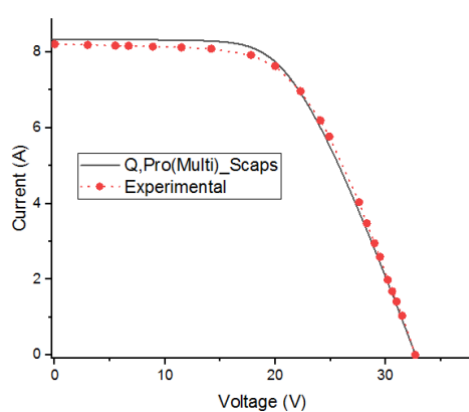**Figure 4.9 :** Experimental data (dotted red line), SCAPS-model (solid black line) for PV module Qpro operating at G=1000 W/m2 T=25 °C (a) I-V characteristic (b) P-V characteristic.

Table 4.3 : Comparisons between simulated and measured P-V curves of each used PV technologies for SCAPS 1-D model..

PV module	technology	G [W/m²]	T [°C]	RMSE [W]	R^2[%]	MPE [%]	Dev [ ]
First Solar FS-272	CdTe	1000	25	1.9974	99.08	-0.1899	-0.0418
Q.Pro 230Wp	Poly C-Si	1000	25	3.5438	99.72	0.0139	0.0029
Q.Smart 95Wp	CIGS	1000	25	3.4960	98.54	0.2873	0.0517

Table 4.3 shows, for each PV module and for a stable given climate conditions, the computed statistical errors. One can notice that the RMSE values are relatively low; ranging between 1.9974W and 3.5438W. Furthermore, the deviations from the measured values are the range that is [-0.0418, 0.0517]. The correlation coefficient values are greater than 98.54 % regardless the technology of the module and the weather conditions. Moreover, the absolute values of the MPE are always less or equal to 0.2873 %. Upon the analysis of these results, it can be concluded that the proposed SCAPS 1-D-based-PV model offers a good performance in predicting the electrical characteristics (i.e., current, voltage, power) of different PV technologies, specially, a PV module having Poly C-Si technology that has the highest correlation values (99.72%) and the lowest *|MPE|* and *|Dev|,* 0.0139 and 0.0029, respectively. Likewise, the obtained static errors of CDTE PV module lead to say that SCAPS 1-D-based-PV model can offer satisfactory prediction for this technology. However, the predicted electrical characteristics of CIGS PV module present the poorest performances compared to the remaining. This has the lowest correlation (98.54%) and the highest *|MPE|* and *|Dev|* (0.2873 and 0.0517, respectively).

4.3 Comparison between Simscape model and SCAPS 1-D model:

(a)   (b)

Figure 4.10 : Experimental data (dotted blue line), SCAPS-model (solid red line) , Simscape-model (solid green line) for PV module FS-272 operating at G=1000 W/m2 T=25 °C (a) I-V characteristic (b) P-V characteristic.

(a)   (b)

Figure 4.11 : Experimental data (dotted blue line), SCAPS-model (solid red line) , Simscape-model (solid green line) for PV module Qsmart operating at G=1000 W/m2 and T=25 °C (a) I-V characteristic (b) P-V characteristic.
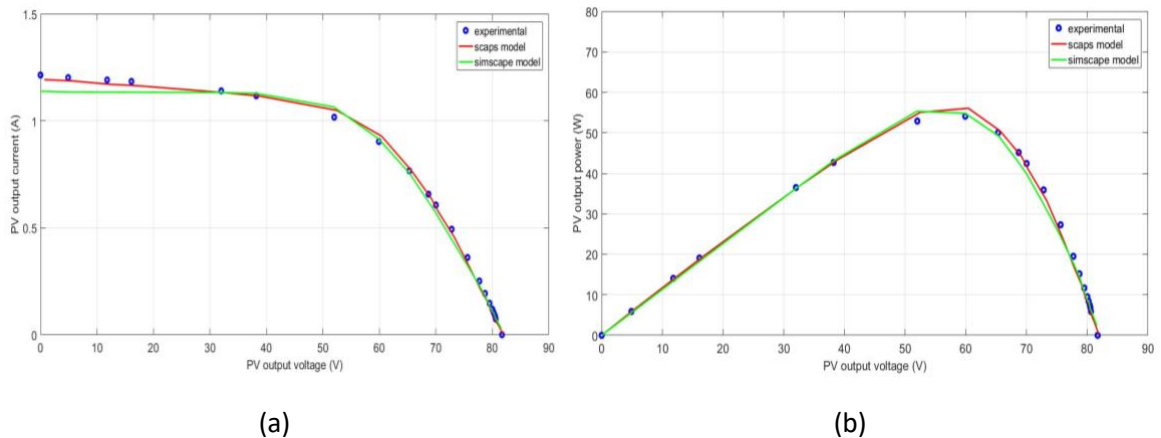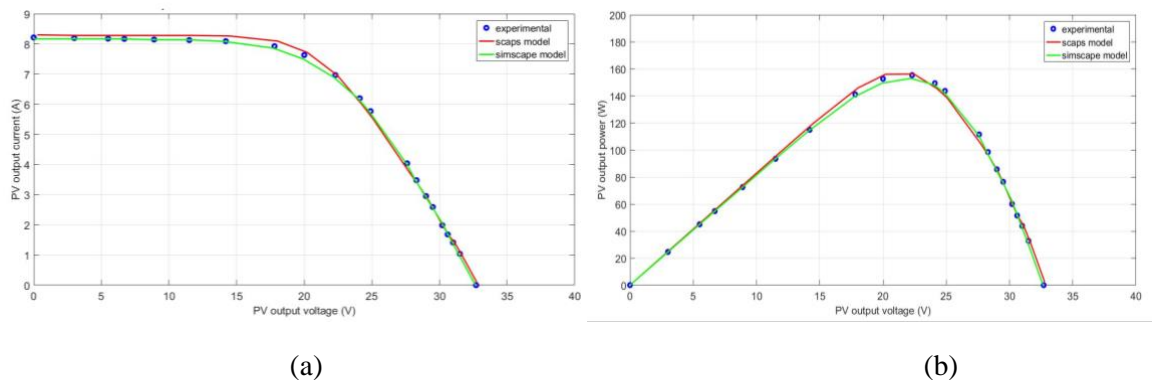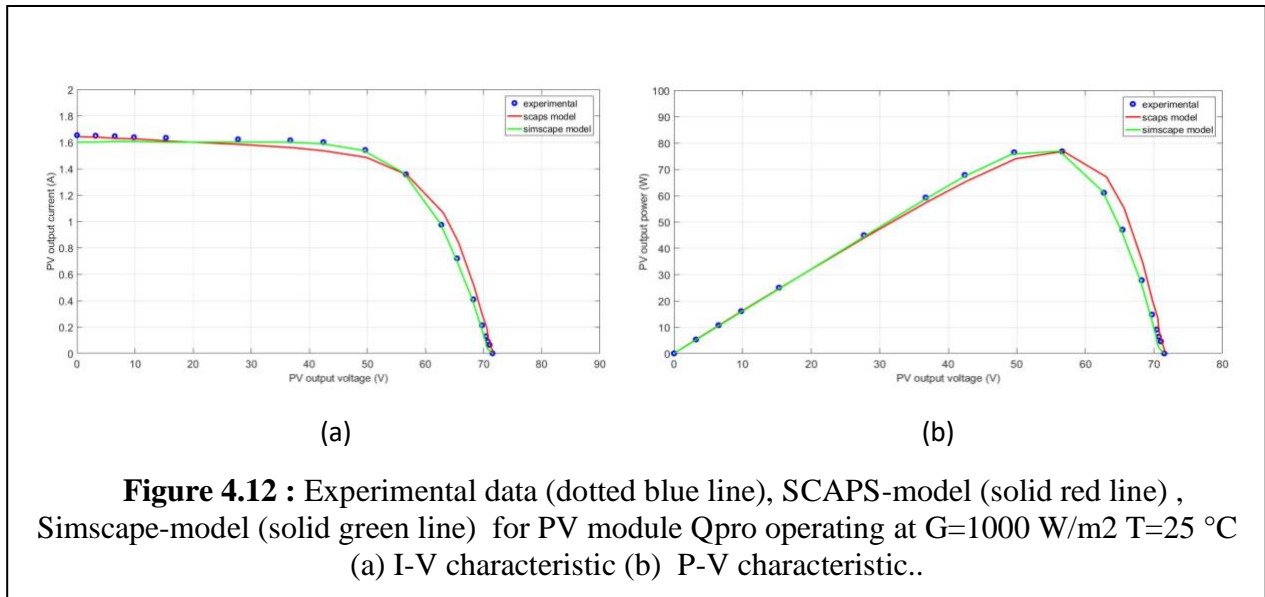
Figure 4.12 : Experimental data (dotted blue line), SCAPS-model (solid red line) , Simscape-model (solid green line) for PV module Qpro operating at G=1000 W/m2 T=25 °C (a) I-V characteristic (b) P-V characteristic..

The three previously shown figures **4.10 to 4.12** represent a comparison between the experimental data (dotted blue line) the SCAPS model (solid red line) and the Simscape-model (solid green line) for each module at G=1000 W/m2 and T=25 °C.

As we notice for Fig **4.10** for FS-272 PV module based CdTe Technology that the agreement between Simscape model and experimental data is better than the agreement between Scaps Model and experimental data .

And for Fig **4.11** for Q.Smart PV module based CIGS Technology the agreement between Simscape model and experimental data surpasses the agreement between Scaps Model and experimental data.

Finally for the Fig **4.12** for Q.Pro PV module based Poly C-Si Technology the agreement between Simscape model and experimental data exeeds the agreement between Scaps Model and experimental data.

Conclusion

Noting the comparisons between the results of the Simscape model and Scaps model with the experimental data for each PV Technology we must conclude that the Simscape model offers a good performance for the modeling of PV module.

General Conclusions

The contribution of this dissertation has been achieved by developing photovoltaic generators (Cell or modules) based on the datasheet parameters to predict the electrical characteristics of different PV technologies: Poly-Crystalline Silicon (Poly C-Si), Copper Indium Gallium Selenide (CIGS) and Cadmium Telluride (CdTe).

The first model has been developed by using the Simscape software as well as a model that uses only the datasheet parameters to calculate the series resistance of each technology. Another PV model has been developed by using SCAPS 1-D software.

The two models have been experimentally tested under different working conditions. The assessment criteria based on four statistical errors have been calculated to precisely evaluate the performance of the Simscape-based-PV model as well as the SCAPS 1-D model in predicting the I-V and P-V characteristics.

The obtained results show that the SCAPS 1-D model offers a satisfactory accuracy of prediction. Whereas, the Simscape-based-PV model offers a superior performance of prediction compared to the SCAPS 1-D model.

On the basis of the promising findings presented in this dissertation, The next stage of our research will be the identification of the exact solar cell area in order to be used in the SCAPS 1-D model for improving its performance.

Références

[1] HANNOUN ABDELKARIM, DJELLAILI BOUDALI, « Modélisation et simulation d'un système photovoltaïque alimentant d'une charge triphasé » MEMOIRE MESTRE(LMD), université Dr.Tahor Moulay de SAIDA, 2015/2016.

[2] SOUHILA AKHMOUM, AGHILAS YAHMI « Réalisation d'une carte de Recherche de point de puissance maximale »MEMOIRE MASTER Université Mouloud Mammeri de Tizi Ouzou, 06/10/2015

[3] ZAHAR SORIA, MAKHLOF CHEYMA « Etude et simulation d'un Générateur photovoltaïque Muni d'un convertisseur MPPT pour une meilleur gestion énergétique » THEME MASTER ACADEMIQUE, université Mohamed Boudiaf-M'sila-2016/2017.

[4] Fondriest Environmental, Inc. "Solar Radiation and Photosynethically Active Radiation." Fundamentals of Environmental Measurements. 21 Mar. 2014. Web. < https://www.fondriest.com/environmental-measurements/parameters/weather/solar-radiation/ >.

[5] AHMED SERRAR, « Etude et Conception des systèmes de recharge solaire pour voiture électrique en Algérie » université du Québec à Trois-Rivières Novembre/2019.

[6] https://www.pveducation.org/pvcdrom/solar-cell-operation/solar-cell-structure

[7] APS News, Alan Chodos April 25, 1954: Bell Labs Demonstrates the First Practical Silicon Solar Cell.

[8] Richter A., Hermle M., Glunz S.W. Reassessment of the limiting efficiency for crystalline silicon solar cells *IEEEJ. Photovolt.* 2013;3:1184–1191 doi: 10.1109/JPHOTOV.2013.2270351..

[9] Sharma P., Goyal P. Evolution of PV technology from conventional to nano-materials. *Mater. Today Proc.* 2020;28:1593–1597. doi: 10.1016/j.matpr.2020.04.846.

[10] Kuczyńska-Łażewska A., Klugmann-Radziemska E., Witkowska A. Recovery of Valuable Materials and Methods for Their Management When Recycling Thin-Film CdTe PV Modules. *Materials.* 2021;14:7836. doi: 10.3390/ma14247836.

[11] Dunlap-Shohl W.A., Zhou Y., Padture N.P., Mitzi D.B. Synthetic approaches for halide perovskite thin films. *Chem. Rev.* 2019;119:3193–3295. doi: 10.1021/acs.chemrev.8b00318.

[12] Peumans P., Yakimov A., Forrest S.R. Small molecular weight organic thin-film photodetectors and solar cells. *J. Appl. Phys.* 2003;93:3693–3723. doi: 10.1063/1.1534621.

[13] https://www.energy.gov/eere/solar/solar-PV-cell-basics

[14] Richard Corkish, in Encyclopedia of Energy, 2004

[15] https://sinovoltaics.com/learning-center/solar-cells/polycrystalline-silicon-cells-production-and-characteristics/

[16] A.E. Dixon, in Solar Energy Conversion II, 1981

[17] Chirilă, A. et al. (2011). "Thin-film solar cells: a review." Progress in PVs: Research and Applications, 19(7), 894-918.

[18] https://www.nrel.gov/pv/cell-efficiency.html

[19]https://www.researchgate.net/figure/Characteristic-I-V-curve-of-a-PV-module_fig1_259996670

[20] Argaw N (2004) Renewable energy water pumping systems handbook. Denver, Colorado.

[21] King DL, Kratochvil JA, Boyson WE. PV array performance model.Sandia National Laboratories, SAND2004-3535; 2004

[22] Course puplised by Y. Baghzouz, "EE 446/646 PV Devices III", http://www.egr.unlv.edu/~eebag/Photovoltaic%20Devices%20III.pdf

[23] https://strageon.gr/en/autonomous-PV-systems

[24] Oriti G, Julian AL (2011) Three-phase VSI with FPGA-based multisampled space vectormodulation. IEEE Trans Ind Appl 47:1813–1820

[25] https://www.cleanenergyreviews.info/blog/2014/8/14/what-is-hybrid-solar

[26] P. A. Basore"Numerical modeling of textured silicon solar cells using PC-1D"Electron Devices, IEEE Transactions on, vol. 37, pp. 337 -343, 1990.

[27] Y.H Khattak Modeling of High Power Conversion Efficiency Thin Film Solar Cells 2019.

[28] SCAPS 3.0, An introduction, K. Decock and M. Burgelman

[29] W. Xuanzhi, High-efficiency Poly C-SiCdTe thin-film solar cells, Sol. Energy, 77(6) (2004) 803-814

[30] Characterization of the Energy Band Diagram of Fabricated SnO2/CdS/CdTe Thin Film Solar Cells R. A. Abdullah, Mohammed A. Razooqi, A. Al-Ajili Published 24 July 2013

[31] Numerical Characterization of Cu(In,Ga)Se2 Solar Cells Using Capacitance-Voltage and Capacitance-Frequency Characteristics Daouda Oubda, M. B. Kebre, Zacharie Koalga Published 20 January 2018.

[32] A Study on the Band Structure of ZnO/CdS Heterojunction for CIGS Solar-Cell Application Hana Sim, Jeongmin Lee, S. Kwon Published 30 April 2015

[33] Sidi Dede, M. , Lamine Ba, M. , Amadou Ba, M. , Ndiaye, M. , Gueye, S. , Sow, E. , Diatta, I. , Diop, M. , Wade, M. and Sissoko, G. (2020) Back Surface Recombination Velocity Dependent of Absorption Coefficient as Applied to Determine Base Optimum Thickness of an n+/p/p+ Silicon Solar Cell. Energy and Power Engineering, 12, 445-458. doi: 10.4236/epe.2020.127027.

[34] Alpaydin, E.: Machine learning: the new AI. MIT press, USA (2016)

[35] LeCun, Y., Bengio, Y., Hinton, G.: Deep learning. Nature 521(7553):436 (2015)

[36] Goodfellow, I., Bengio, Y., Courville, A.: Deep learning. MIT Press, New York (2016)

[37] Haque, A., Bharath, K.V.S., Khan, M.A., Khan, I., Jaffery, Z.A.: Fault diagnosis of PV modules. Energy Sci Eng 7(3), 622–644 (2019)

[38] Köntges, M., Kurtz, S., Jahn, U., Berger, K., Kato, K., Friesen, T., et al.: Review of failures of PV modules. In: IEA PVPS Task, p. 13 (2014)

[39] Yagi, Y., Kishi, H., Hagihara, R., Tanaka, T., Kozuma, S., Ishida, T., et al.: Diagnostic technology and an expert system for PV systems using the learning method. Solar Energy Mater Solar Cells 75, 655–663 (2003)